



Potential energy curves, turning points, Franck–Condon factors and r -centroids for the astrophysically interesting S_2 molecule

Ramon S. da Silva¹ · Maikel Y. Ballester¹

Received: 14 August 2019 / Accepted: 1 October 2019 / Published online: 8 October 2019
© Springer Nature B.V. 2019

Abstract We have theoretically studied the seven lowest triplet states of the disulfur species. For such investigations, analytical potential energy curves (APECs) for $X^3\Sigma_g^-$ ground and $A'^3\Delta_u$, $A^3\Sigma_u^+$, $B''^3\Pi_u$, and $B^3\Sigma_u^-$ excited electronic states were constructed within the extended Hartree–Fock approximate correlation energy (EHFACE) model by Varandas. Once that these analytical representations are obtained, nuclear properties, such as vibrational energies, classical turning points, and spectroscopic constants were calculated. Particularly, comparisons between these vibrational levels with those obtained via the Rydberg–Klein–Rees (RKR) methodology as implemented in Le Roy’s RKR1 code are reported. The impact of tight d augmented correlation consistent basis on the energies and frequencies is shown. We also re-examined the vibronic (vibration–electronic) transition parameters as Franck–Condon (FC) factors and r -centroids for the bands of the $B''^3\Pi_u-X^3\Sigma_g^-$, $B^3\Sigma_u^-X^3\Sigma_g^-$, $C^3\Sigma_u^-X^3\Sigma_g^-$, and $D^3\Pi_u-X^3\Sigma_g^-$ systems of the S_2 molecule. The vibrational levels and turning points of the two Rydberg states $C^3\Sigma_u^-$ and $D^3\Pi_u$ were computed only with the RKR method. Our results can be employed in rationalizations of astrochemical and astrophysical observations.

Keywords Potential energy curves · FC factors · r -centroids · Vibrational levels · S_2 molecule

Electronic supplementary material The online version of this article (<https://doi.org/10.1007/s10509-019-3656-3>) contains supplementary material, which is available to authorized users.

✉ R.S. da Silva
ramonshowsa@gmail.com
M.Y. Ballester
maikel.ballester@ufjf.edu.br

¹ Departamento de Física, Universidade Federal de Juiz de Fora, Juiz de Fora, MG, Brazil

1 Introduction

There is a great astrophysical interest in sulfur-bearing molecules since these species have been detected in the interstellar medium (ISM) and star-forming regions (Wakelam et al. 2004). Over the years, gas-phase sulfur compounds have become the target of many studies due to its chemistry and physical properties (Anderson et al. 2013; Lucas et al. 1995; Vidal et al. 2017; Wakelam et al. 2004, 2011). In this scenario, neutral molecules such as OCS, H_2S , SO, SO_2 , NS, and CS might represent the most probable reservoirs for S atoms in the ISM (Wakelam et al. 2011; van der Tak et al. 2003). According to Anderson et al. (2013), the dissociation of H_2S molecules plays an important role in the formation of other S-containing species, for instance, CS_2 , H_2S_2 , and S_n . Druard and Wakelam (2012) pointed out that, for temperatures higher than those found in dark clouds (around 10 K), sulfur was also converted into other forms (e.g., H_2S_3).

Experimental simulations with ultraviolet (UV) and soft X-ray irradiation show that solid H_2S found in the interstellar ices can form S_2 , HS_2 , and S-polymers like S_8 during warm-up of their photolyzed ices (Jiménez-Escobar and Caro 2011; Jiménez-Escobar et al. 2012). Accordingly, the results of these experiments could help explain the detection of disulfur in comets. It is worth mentioning that S_2 molecules have been identified in many comets (Laffont et al. 1998). The first of such observations occurred in the UV spectra of the comet IRAS-Araki-Alcock (C/1983 H1) performed with the help of the International Ultraviolet Explorer (IUE) space observatory (Ahearn et al. 1983; Saxena et al. 2003). Observations of S-containing molecules have also been reported in other comets as Hyakutake (C/1996 B2), Ikeya-Zhang (C/2002 C1), and Lee (C/1999 H1) (Reylé and Boice 2003; Feldman et al. 1999).

In 1994, fragments of comet Shoemaker-Levy 9 (hereafter simply SL-9) collided with Jupiter's atmosphere (Mauerris and Cravens 2001). After impact, a series of investigations revealed large amounts of disulfur in its ionosphere (Noll et al. 1995; Mauerris and Cravens 2001). Experimentally, electronic transitions like $B^3\Sigma_u^- - X^3\Sigma_g^-$ were identified in the range covering the wavelength region of 2400 to 3200 Å (Noll et al. 1995).

To explain the appearance of disulfur in the UV spectra of the comet Halley, the following reaction mechanism was proposed by Saxena and Misra (1995):



with both species in their ground electronic states. Subsequently, a high level ab initio theoretical investigation presented by Woon (2007) showed that not only this mechanism but also those involving acetylene (C_2H_2) could contribute to the formation of S_2 molecule in comets. However, another important result verified by them is that, energetically, the reactions with C_2H_4 are more favorable sources of S_2 than the corresponding with C_2H_2 .

Potential energy curves (PECs) as well as its molecular properties like spectroscopic parameters and rovibrational levels for the ground triplet $X^3\Sigma_g^-$ and excited singlet $a^1\Delta_g$ states of S_2 molecule were explored by Wei et al. (2016). Similarly, the six lowest states of sulfur dimer have been recently investigated by Qin et al. (2019). There, experimental and theoretical techniques were used to obtain accurate spectroscopic parameters.

Furthermore, a series of researches, both theoretical and experimental, were developed with the purpose of to characterize the vibronic transitions, i.e., vibration-electronic transitions for S_2 molecule (Anandaraj et al. 1992; Anderson et al. 1979; Sarka et al. 2019; Green and Western 1996; Tanaka and Ogawa 1962; Herman and Felenbok 1963; Smith and Liszt 1971; Verma and Mahajan 1988; Smith and Hopkins 1981; Gerasimova et al. 2002; Qin et al. 2019; Meyer and Crosley 1973). For example, Anandaraj et al. (1992) calculated the Franck–Condon (FC) factors and r -centroids for some bands of the $C^3\Sigma_u^- - X^3\Sigma_g^-$ and $D^3\Pi_u - X^3\Sigma_g^-$ systems. Their results suggest that both bands are blue degraded bands. Using flash photolysis experiments Carleer and Colin (1970) studied 28 vibrational bands of the $f^1\Delta_u - a^1\Delta_g$ transition. Previously, Barrow and Du Parcq (1968) also investigated the vibronic transition of this same system using a discharge tube. In addition, a second band system ($g^1\Delta_u - a^1\Delta_g$) was observed by them in UV region. Spectroscopic parameters were experimentally determined in all cases.

The UV absorption spectrum of sulfur dimer is dominated by the $B^3\Sigma_u^- - X^3\Sigma_g^-$ Schumann–Runge transition of

the isovalent O_2 molecule (Green and Western 1996). Smith and Hopkins (1981) employing a CW helium-cadmium laser suggest that this band is expected in the red degraded region. According to Spencer et al. (2000) this band system was detected in Io's Pele plume. This region is known by a high volcanic activity; thus, it can be inferred that disulfur is a product of other reactions taking place there.

Theoretically, oscillator strengths, transition probabilities, and radiative lifetimes for the $B^3\Sigma_u^- - X^3\Sigma_g^-$ and $B''^3\Pi_u - X^3\Sigma_g^-$ band systems were computed by Pradhan and Partridge (1996). In the same way, Smith and Liszt (1971) calculated RKR FC factors and r -centroids in different diatomic systems (NH, SiH, SiD, SO, and S_2). Among the selected species the $B^3\Sigma_u^- - X^3\Sigma_g^-$ transition of S_2 was examined. This band system has also been investigated by Herman and Felenbok (1963).

Yet, from an experimental point of view, the observations of S_2 (B-X) chemiluminescence has been previously documented through collisions between alkaline earth atoms with S_2Cl_2 (Engelke and Zare 1977) and SCl_2 (Wright and Balling 1984). An important contribution was given by Anderson et al. (1979) when Franck–Condon factors were estimated from intensity measurements, using a frequency-doubled tunable dye laser.

Laser-induced fluorescence (LIF) was used by Green and Western (1996) to provide a complete deperturbation analysis of the $B^3\Sigma_u^-$ ($v = 0-6$) and $B''^3\Pi_u$ ($v = 2-12$). In turn, Narasimham and his co-workers have observed spin-allowed transitions such as $B'^3\Pi_g - A^3\Sigma_u^+$ and $B'^3\Pi_g - A'^3\Delta_u$ (Narasimham et al. 1976a,b). Lee and Pimentel (1979) employing experimental techniques demonstrated that S_2 can be produced at low temperatures ($T < 25$ K) within other sulfur-bearing species. For all these reasons presented, there is a notable interest in the molecular properties of neutral sulfur dimer species as well as its spin-allowed vibronic transitions.

Then, motivated by this research, in this paper, we present a revised and refined study involving only vibronic transitions of the triplet electronic states. To achieve these goals, analytical potential energy curves (APECs) for the ground $X^3\Sigma_g^-$ and excited electronic states $A'^3\Delta_u$, $A^3\Sigma_u^+$, $B''^3\Pi_u$, and $B^3\Sigma_u^-$ have been constructed by fitting ab initio points taken from Sarka et al. (2019). There, the electronic energies were computed using internally contracted multireference configuration interaction (MRCI-F12) level of theory and aug-cc-pVQZ (AVQZ) Dunning basis set. In the fitting, an analytical form proposed by Varandas namely the extended Hartree–Fock approximate correlation energy (EHFACE) model was adopted (Varandas and Silva 1992). Additionally, to evaluate the effect of tight d functions to the correlation consistent sets, quantum-chemical calculations at MRCI with Davidson modification (Q) level of theory in association with aug-cc-pV(5+d)Z Dunning basis set

were carried out. For comparisons, the vibrational levels and turning points for these states have been calculated employing the Rydberg–Klein–Rees (RKR) method. This methodology essentially extracts diatomic potentials from the spectroscopic measure.

After these processes, we calculated Franck–Condon (FC) factors and r -centroids for the vibronic (vibration–electronic) $B''^3\Pi_u-X^3\Sigma_g^-$, $B^3\Sigma_u^-X^3\Sigma_g^-$, $C^3\Sigma_u^-X^3\Sigma_g^-$, and $D^3\Pi_u-X^3\Sigma_g^-$ transitions. We also compared our results with those data available in the literature and discussed their astrophysical importance. We believe that the present study provides motivation for a search of S_2 triplet bands. In addition, our results can serve as a benchmark in the spectral analysis of future predictions.

The paper is organized as follows. Section 2 contain a detailed description of the models used by us to describe our potential energy curves. A discussion about technical details for RKR methodology and a brief survey of EHFACE method are also presented. The results are gathered in Sect. 3 and the conclusions are given in the last section.

2 Models for the potential energy curves

2.1 RKR method

In this work, we construct the rotationless potential energy curves for triplet states of disulfur molecule using the Rydberg–Klein–Rees (RKR) methodology (Rydberg 1931, 1933; Klein 1932; Rees 1947) as implemented in Le Roy's RKR1 package (Le Roy 2017). For a given electronic state, the rovibrational level energies are calculated based on a Dunham's expansion energy (Dunham 1932):

$$T_{v,J} = T_e + \sum_{l,m} Y_{l,m} \left(v + \frac{1}{2} \right)^l [J(J+1)]^m \quad (3)$$

where v and J are the vibrational and rotational quantum numbers, while T_e is the value of minimum electronic energy referred to the well depth for the ground electronic state (here $X^3\Sigma_g^-$). Notice that in this equation $Y_{l,m}$ represents the known Dunham coefficients. These coefficients are easily identifiable as the spectroscopic parameters often used in diatomic molecule studies, e.g.,

$$\begin{cases} Y_{1,0} \approx \omega_e; & Y_{2,0} \approx -\omega_e x_e, \\ Y_{0,1} \approx B_e; & Y_{1,1} \approx -\alpha_e. \end{cases}$$

This procedure has been extensively applied in the study of other diatomic systems (Whang et al. 2004; Ashman et al. 2012; da Silva et al. 2008). More details of the RKR method can be found elsewhere (Le Roy 2017).

To obtain an accurate description of vibration–rotation energies and other properties it is very important to make

a refined selection of the spectroscopic parameters. However, da Silva et al. (2008) have pointed out that in some cases RKR method can lead us to significant differences from those “exact” vibrational energies. Such inaccuracy is attributed to the anharmonicity of the PEC. In this work, we kept the vibrational quantum numbers below 10. Thus we avoid errors when v and J become larger. We stress that the set of measured spectroscopic parameters used in the input data file were taken from Huber and Herzberg (1979) for $X^3\Sigma_g^-$ and $D^3\Pi_u$, Barrow et al. (1969) for $C^3\Sigma_u^-$, Narasimham et al. (1976b) for $A'^3\Delta_u$, Narasimham et al. (1976a) for $A^3\Sigma_u^+$, and Patinõ and Barrow (1982) for $B''^3\Pi_u$.

2.2 EHFACE potential method

The analytical PECs for $X^3\Sigma_g^-$ ground and $A'^3\Delta_u$, $A^3\Sigma_u^+$, $B''^3\Pi_u$, and $B^3\Sigma_u^-$ excited triplet electronic states were constructed based on the Extended Hartree–Fock Approximate Correlation Energy (EHFACE) model (Varandas and Silva 1992). In this technique, the total interaction energy is written as

$$V(R) = V_{\text{EHF}}(R) + V_{dc}(R). \quad (4)$$

The equations $V_{\text{EHF}}(R)$ and $V_{dc}(R)$ denote the extended Hartree–Fock (EHF) and the two-body dynamical correlation (dc) energy terms, respectively. More details from this expansion are found elsewhere (Ballester and Varandas 2005; da Silva and Ballester 2018; Song et al. 2018; Varandas and Silva 1992). Within the EHFACE model, the correct asymptotic limits $R \rightarrow \infty$ and $R \rightarrow 0$ are warranted. Based on this methodology, the EHFACE model is employed to fit ab initio points extracted from Supplementary Material of Sarka et al. (2019). The parameters of Eq. (4) have been fitted using the least-squares method such as mentioned by da Silva and Ballester (2018). For further discussions about other analytical forms of diatomic potentials, we suggest seeing (Araújo et al. 2019).

Statistically, to evaluate the fitting quality of the ab initio electronic energies we calculate the root-mean-square deviation. This quantity, denoted herein by RMSD, is defined as

$$\text{RMSD} = \left[\frac{1}{N} \sum_{i=1}^N (V_{\text{ab initio}} - V)^2 \right]^{1/2} \quad (5)$$

where V is obtained via EHFACE model. RMSD is used to measure the differences between values predicted by a model (V) and the ab initio data ($V_{\text{ab initio}}$). This error criterion is widely used to evaluate the analytical or numerical molecular potential energy constructed. Moreover, as it is already known, the smaller RMSD values represent better performance, and a higher error reflects worst stability. So, these parameters were used to judge how well the model reproduces the ab initio data.

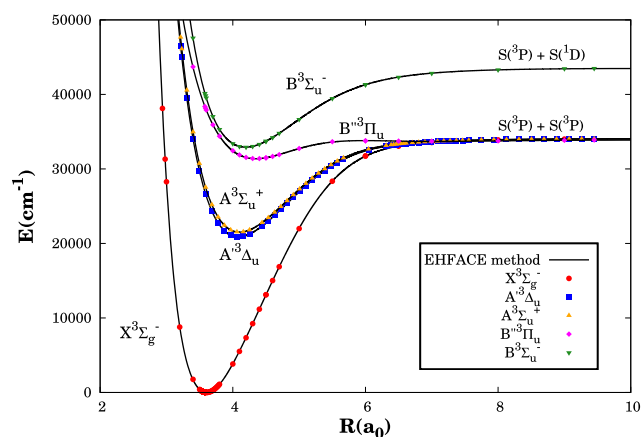


Fig. 1 Potential energy curves for ground and four triplet excited states of S_2 molecule. Ab initio points from Sarka et al. (2019) are also represented

3 Results and discussion

3.1 Energetic aspects and spectroscopic parameters

We start this discussion showing in Fig. 1 a view of our potential energy curves computed through EHFACE procedure (solid lines). For comparison, ab initio energies from Sarka et al. (2019) are incorporated in these plots. All fitted parameters together with RMSD values for the studied cases are collected in Table I on the Supplementary Material. The EHFACE model leads to deviations of the magnitudes of 0.05 kcal/mol. These values are less than the threshold of chemical accuracy (1.0 kcal/mol), therefore we can conclude that our results reproduce with accuracy and robustness those electronic energies. In recent investigations of disulfur, similar RMSD values were calculated by Zhang et al. (2015a,b) for singlet electronic states $a^1\Delta_g$ and $b^1\Sigma_g^+$. There, Zhang and co-workers followed a similar procedure to model the diatomic interaction energies.

Notice that the triplet electronic states $X^3\Sigma_g^-$, $A^3\Delta_u$, $A^3\Sigma_u^+$, $B''^3\Pi_u$ converge to the dissociation limit $S(^3P) + S(^3P)$, while the excited state $B^3\Sigma_u^-$ dissociates to $S(^3P) + S(^1D)$. At this moment, it is important to remark that the relative energy calculated between $^3P + ^3P$ and $^3P + ^1D$ dissociation limit present a difference of 9359 cm^{-1} (or 26.7 kcal/mol). This value is 120 cm^{-1} larger than the experimental measurement of 9239 cm^{-1} (Xing et al. 2013, and the references therein).

Our next step was to examine the spectroscopic quantities (T_e , R_e , ω_e , $\omega_e x_e$, α_e , B_e , D_0 , D_e) derived from the APECs. The obtained values are gathered in Table 1. Column one of this table indicates the kind of method employed, whereas the electronic state of S_2 is given in column two. The values of the minimum to minimum electronic energy, T_e , are presented in the third column and the bond distances (R_e) are listed in fourth column. The fifth and sixth columns of

Table 1 show the harmonic and anharmonic vibrational frequencies, respectively. The last four columns contain the results for the vibration–rotation interaction constant (α_e), the rotational constant (B_e), the dissociation energy (D_0), and the well depth (D_e). The diatomic dissociation energy has been calculated using the approximation

$$D_0 = D_e - \frac{\omega_e}{2}; \quad (6)$$

we also stress that the values of spectroscopic parameters $\omega_e x_e$ and α_e can be affected by ω_e and B_e .

Still in the same table, we included also some results obtained from *state-of-the-art* calculations (Sarka et al. 2019; Pradhan and Partridge 1996; Xing et al. 2013) and experimental data (Huber and Herzberg 1979; Narasimham et al. 1976a,b; Patinõ and Barrow 1982).

As results, the predicted values for ω_e are 14.6, 10.6, 11.9, 22.4, and 29.3 cm^{-1} different from the experimental data (725.6, 488.1, 482.1, 335.2, and 434.0 cm^{-1}) for the $X^3\Sigma_g^-$, $A^3\Delta_u$, $A^3\Sigma_u^+$, $B''^3\Pi_u$, and $B^3\Sigma_u^-$ states of S_2 , respectively. As can be seen from this table, the equilibrium bond length values are well reproduced by our analytical representations. For example, the APECs estimated equilibrium distances deviate by 0.0359, 0.0307, 0.0393, 0.0400, and 0.0935 a_0 from the experimental values in each electronic state analyzed.

In particular, when comparing our results for the ground electronic state with those from Sarka et al. (2019) the deviations of the present R_e , ω_e , $\omega_e x_e$, α_e , and B_e are only 0.0041 a_0 , 9.60, 1.43, 0.0003, and 0.0007 cm^{-1} . Similarly, small differences of magnitude 0.023 (0.031) a_0 , 8.8 (13.9), 0.90 (0.83), 0.0003 (0.0002), and 0.0034 (0.0053) cm^{-1} are obtained compared to theoretical data reported by Pradhan and Partridge (1996) (Xing et al. 2013). The dissociation energy, D_0 , calculated for the ground state is 1934.9 cm^{-1} , less than the experimental one (Huber and Herzberg 1979). On the other hand, this value is 352.7 cm^{-1} larger than those reported by Sarka et al. (2019). From an experimental point of view this reported difference is significantly large.

Concerning the excited state $A^3\Delta_u$, reference theoretical data ($T_e = 21360.5\text{ cm}^{-1}$, $R_e = 4.0578\text{ a}_0$, $\omega_e = 490.7\text{ cm}^{-1}$, $\omega_e x_e = 2.49\text{ cm}^{-1}$, $\alpha_e = 0.00139\text{ cm}^{-1}$, $B_e = 0.2285\text{ cm}^{-1}$, $D_0 = 14228.4\text{ cm}^{-1}$) are taken from Xing et al. (2013). As can be seen from the table, our estimated value of anharmonic constant ($\omega_e x_e$) is almost the double of their. In addition, the harmonic vibrational frequency and the dissociation energy are 13.1 and 1326.4 cm^{-1} below of their. In relation to $A^3\Sigma_u^+$ electronic state similar deviations are observed.

For the $B^3\Sigma_u^-$ state, the spectroscopic properties R_e and $\omega_e x_e$ overestimate by 0.0009 a_0 and 1.29 cm^{-1} the theoretical values from Sarka et al. (2019), while the remaining parameters T_e , ω_e , α_e , B_e and D_e are underestimated by

Table 1 Spectroscopic parameters compared with available data in the literature for the S_2 molecule

State	Method	T_e (cm^{-1})	R_e (a_0)	ω_e (cm^{-1})	$\omega_e x_e$ (cm^{-1})	α_e (cm^{-1})	B_e (cm^{-1})	D_0 (cm^{-1})	D_e (cm^{-1})
$X^3\Sigma_g^-$	This work	0	3.6059	711.0	3.71	0.00182	0.2893	33668.0	34023.5
	Theo. ^a	0	3.6018	720.6	2.28	0.00152	0.2900	34020.7	–
	Theo. ^b	0	3.5829	719.8	2.81	0.00148	0.2927	35424.7 ± 242.0	–
	Theo. ^c	0	3.5749	724.9	2.88	0.00159	0.2946	35560.9	–
	Theo. ^d	0	3.5679	727.4	2.84	0.00160	0.2958	35625.5	–
	Theo. ^e	0	3.5753	726.0	2.81	–	0.2945	36230.4	–
	Exp. ^e	0	–	714.0 ± 12.0	–	–	–	–	–
	Exp. ^f	0	3.5700	725.6	2.84	0.00157	0.2954	35602.9	–
$A'^3\Delta_u$	This work	20882.7	4.0860	477.6	4.34	0.00216	0.2253	12902.0	13140.8
	Theo. ^c	21360.5	4.0578	490.7	2.49	0.00139	0.2285	14228.4	–
	Theo. ^e	21509.0	4.0591	491.0	2.71	–	0.2286	14792.2	–
	Exp. ^e	21960.0 ^g	–	–	–	–	–	–	–
	Exp. ^h	21356.9 ^g	4.0553 ⁱ	488.1	2.51	–	–	–	–
$A^3\Sigma_u^+$	This work	21508.3	4.1022	470.2	4.41	0.00219	0.2235	12280.1	12515.2
	Theo. ^c	21918.2	4.0723	482.7	2.59	0.00150	0.2270	13631.5	–
	Theo. ^e	22147.0	4.0723	486.0	2.71	–	0.2271	14405.1	–
	Exp. ^e	22839.0 ^g	–	–	–	–	–	–	–
	Exp. ^j	21971.4 ^g	4.0629 ⁱ	482.1	2.56	0.00140	0.2248	–	–
$B''^3\Pi_u$	This work	31518.5	4.3485	312.8	4.70	0.00350	0.1989	2348.6	2505.0
	Theo. ^a	31373.0	4.3558	306.4	4.0	0.00210	0.1980	2498.5	–
	Theo. ^b	31254.7	4.3085	325.4	4.52	0.00261	0.2026	4161.9 ± 332.0	–
	Theo. ^c	31326.9	4.2620	337.8	0.293	0.00093	0.2080	5639.4	–
	Exp. ^k	31070.0	–	335.2	4.50	0.00280	0.2100	–	–
$B^3\Sigma_u^-$	This work	32811.4	4.1942	404.7	3.87	0.00220	0.2138	10368.8	10571.1
	Theo. ^a	32911.0	4.1933	408.1	2.58	0.00170	0.2140	10575.7	–
	Theo. ^b	31803.1	4.1007	434.0	2.54	0.00198	0.2234	12784.2 ± 332	–
	Theo. ^c	31967.3	4.0997	433.6	2.67	0.00166	0.2240	13720.2	–
	Exp. ^f	31835.0	4.1007	434.0	2.75	0.00230	0.2239	–	–
$C^3\Sigma_u^-$	Exp. ^l	55581.7	3.4204	829.1	3.34	0.00130	0.3219	–	–
$D^3\Pi_u$	Exp. ^f	58518.3	3.4959	793.8	4.00	–	0.3059	–	–

^aSarka et al. (2019) ^bPradhan and Partridge (1996) ^cXing et al. (2013) ^dWei et al. (2016) ^eQin et al. (2019) ^fHuber and Herzberg (1979)
^g T_0 value ^hNarasimham et al. (1976b) ⁱ r_0 value ^jNarasimham et al. (1976a) ^kPatinõ and Barrow (1982) ^lBarrow et al. (1969)

99.6, 3.4, 0.0005, 0.0002, and 4.6 cm^{-1} . Comparing our results computed with those experimental, R_e , ω_e , and $\omega_e x_e$ deviate 0.0935 a_0 , 29.3 cm^{-1} , and 1.12 cm^{-1} . Note that the theoretical results reported by Pradhan and Partridge (1996) and Xing et al. (2013) are closer to the experimental ones (Huber and Herzberg 1979).

The largest discrepancies appear, probably, when we check the values of the transition electronic energy (T_e) of the four triplet electronic states referred to the ground state $X^3\Sigma_g^-$. Our model points out deviations of T_e from the experiments (Huber and Herzberg 1979; Narasimham et al. 1976a,b; Patinõ and Barrow 1982) by 2.22%, 2.10%, 1.44%, and 3.06% for $A'^3\Delta_u$, $A^3\Sigma_u^+$, $B''^3\Pi_u$, and $B^3\Sigma_u^-$, respectively. The accuracy of T_e is quite important mainly if rovi-

brational levels are calculated using a Dunham expansion (see Eq. (3)).

To conclude this section, we must emphasize that the spectroscopic parameters employed to construct vibrational levels using RKR method of $C^3\Sigma_u^-$ and $D^3\Pi_u$ electronic states were collected from Barrow et al. (1969) and Huber and Herzberg (1979), respectively. These values are listed in Table 1. Usually, the quality of potential energy curves for species formed by S atoms and its corresponding spectroscopic parameters are sensitive to many factors. For instance, the convergence of the wave function in a multi-reference configuration interaction (MRCI) calculation depends heavily on the choice of molecular orbitals (MOs) used in defining the configurations. However, we focus on

Table 2 Spectroscopic parameters for the S₂ molecule calculated by the two different fits (FIT1 and FIT2)

State	Method	T_e (cm ⁻¹)	R_e (cm ⁻¹)	ω_e (cm ⁻¹)	$\omega_e x_e$ (cm ⁻¹)	α_e (cm ⁻¹)	B_e (cm ⁻¹)	D_0 (cm ⁻¹)	D_e (cm ⁻¹)
$X^3\Sigma_g^-$	FIT1	0	3.6059	711.0	3.71	0.00182	0.2893	33668.0	34023.5
	FIT2	0	3.5875	724.5	3.70	0.00180	0.2917	35071.5	35433.7
$A^3\Sigma_u^+$	FIT1	21508.3	4.1022	470.2	4.41	0.00219	0.2235	12280.1	12515.2
	FIT2	21899.3	4.0790	481.0	3.10	0.00206	0.2256	13894.2	14134.7
$B^3\Sigma_u^-$	FIT1	32811.4	4.1942	404.7	3.87	0.00220	0.2138	10368.8	10571.1
	FIT2	31810.6	4.1340	455.5	4.02	0.00208	0.2197	12658.7	12886.4

effects associated with tight d augmented correlation consistent basis sets on the structure of S-bearing molecules. In this sense, a large number of theoretical studies have been reported in the literature (Wilson and Dunning 2003; Bell and Wilson 2004; Wang and Wilson 2005).

As previously described the set of ab initio energies from Sarka et al. (2019) does not include the family of correlation consistent basis sets aug-cc-pV($X + d$)Z. Therefore, based on the literature, we believe that to perform ab initio calculations employing these basis sets the quality and efficiency of our calculated molecular properties for S₂ could improve. To test this hypothesis we perform novel ab initio calculations only using aug-cc-pV(5 + d)Z basis set of Dunning. The details of these calculations are given in the next section.

3.2 Electronic structure calculations

In the present work, ab initio calculations for the electronic states $X^3\Sigma_g^-$, $A^3\Sigma_u^+$, and $B^3\Sigma_u^-$ were performed by means of the MOLPRO program package (Werner et al. 2012). Once obtained these interaction energies the same methodology described in Sect. 2.2 was adopted. After this procedure we calculated the molecular properties of selected electronic states. The point group of the S₂ is $D_{\infty h}$, but due to limitations of the procedure, we adopted D_{2h} subgroup of $D_{\infty h}$ point group in the calculations. The correlating relationships of irreducible representations between D_{2h} and $D_{\infty h}$ is well documented in Xing et al. (2013), Wei et al. (2016), Qin et al. (2019).

Referent to molecular orbitals, for convenience we have followed the same method reported by Xing et al. (2013), Qin et al. (2019), i.e., 12 electrons for sulfur dimer distributed into eight MOs (2 A_g , 1 B_{3u} , 1 B_{2u} , 2 B_{1u} , 1 B_{2g} , 1 B_{3g}). In all cases studied, at a given internuclear distance, the interaction energies were computed at MRCI level of theory including the Davidson correction (MRCI+Q) (Langhoff and Davidson 1974) using the full valence complete active space-self consistent field (CASSCF) wave function as the reference.

For the S atom, we have used the Dunning correlation consistent basis set aug-cc-pV(5 + d)Z (AV(5 + d)Z) family

of basis sets, which contains an additional tight d function to partially ameliorate a known SCF-level deficiency in the AVXZ sets for second-row elements (Dunning et al. 2001). Lastly but not least, intervals of 0.025 a_0 in the internuclear distance ranging from 1.0 to 15.0 a_0 were used to explore the PECs.

To illustrate an improve interpretation of data it is important to mention that from now our fitting using ab initio electronic energies from Sarka et al. (2019) will be called “FIT1”. A second analytical fit “FIT2” corresponds to our MRCI+Q calculations and AV(5 + d)Z basis set. All fitted parameters together with RMSD values for the FIT2 are listed in Table II on the Supplementary Material.

Within such a framework, the new potential energy curves as a function of internuclear distances are shown in Fig. 2. Notice that in each case the zero of energy match to well depth. The experimental RKR data points are also included. Figure 2(c) exhibits the curve for the ground electronic state of the S₂ molecule extracted from the double many-body expansion (DMBE) potential energy surface for ground state HS₂ (Song and Varandas 2011). In their work, the analytical form employed to model two-body fragments is identical to the one used here.

As can be seen, there is an excellent agreement between not only the FIT2 and the RKR potentials but also FIT2 and the APEC reported by Song and Varandas (2011). Yet, for all cases, clearly, large differences are visualized in the intermediate and long-range regions ($R > 4a_0$). It means that the impact of tight d functions upon S₂ increase the well depth. As a consequence, the molecular properties of disulfur seemingly are very sensitive for the aug-cc-pV($X + d$)Z family of basis sets.

In Table 2 are gathered the spectroscopic parameters obtained for both fittings. The vibrational harmonic frequency for the electronic ground state increases to 13.5 cm⁻¹. It differs by 1.1 cm⁻¹ from the experimental measure (Huber and Herzberg 1979). Our results for the $X^3\Sigma_g^-$ predict a relative difference of 0.0175 a_0 in the equilibrium geometry and underestimate the dissociation energy in the approach ~ 531.4 cm⁻¹. Concerning to FIT1, the well depth (D_e^{FIT2}) obtained overestimates (D_e^{FIT1}) by approximately

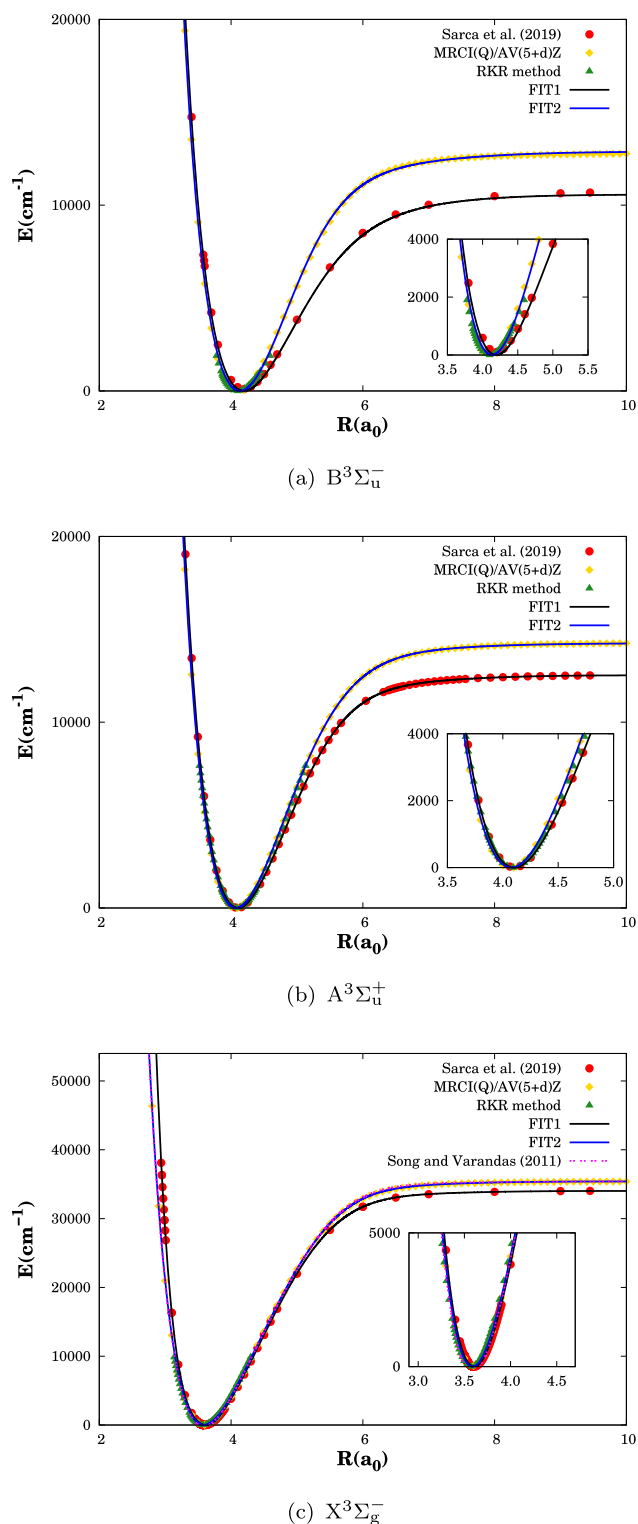


Fig. 2 Overview of the present study of the (a) $B^3\Sigma_u^-$, (b) $A^3\Sigma_u^+$, and (c) $X^3\Sigma_g^-$ states of S_2 molecule. Ab initio points from Sarca et al. (2019) are depicted by \bullet , while our electronic energies calculated at MRCI(Q)/AV(5 + d)Z level of theory are showed by \blacklozenge . \blacktriangle represents experimental RKR data points. The solid red curves are the results of FIT1. On the other hand, the blue ones illustrate FIT2. For comparison, in (c) we add the PEC for ground electronic state (dashed magenta) extracted from Song and Varandas (2011)

1400 cm^{-1} . It can easily be visualized in Fig. 2(c). Upon energetically comparing FIT1 and FIT2 they disagree in the repulsive part of the potential, i.e., at the internuclear distances below R_e .

Analyzing Table 2 and Fig. 2(b), we found for $A^3\Sigma_u^+$ state, values of R_e^{FIT2} , B_e^{FIT2} , ω_e^{FIT2} , and D_e^{FIT2} of $4.0790a_0$, 0.2256 cm^{-1} , 481.0 cm^{-1} , and 14134.7 cm^{-1} , respectively. These values agrees excellently with the experimental data from Narasimham et al. (1976a). Unfortunately, an important constant, D_0 , was not experimentally evaluated by them. A salient feature here is that T_e^{FIT2} is 72.1 cm^{-1} below T_e^{exp} . (see Table 1), while T_e^{FIT1} is 463.1 cm^{-1} .

The same trend is observed when analyzing the $B^3\Sigma_u^-$ state of disulfur molecule (Table 2 and Fig. 2(a)). In relation to T_e^{FIT1} , there is an improvement in the value of dissociation energy of 2289.9 cm^{-1} . Looking into the other spectroscopic parameters aiming to judge the quality of the FIT2, we find that the differences from the experimental data are 24.4 cm^{-1} for T_e^{FIT2} , $0.0333a_0$ for R_e^{FIT2} , 0.0042 cm^{-1} for B_e^{FIT2} , 21.5 cm^{-1} for ω_e^{FIT2} , and 1.27 cm^{-1} for $\omega_e x_e^{\text{FIT2}}$.

In summary, our best spectroscopic constants are predicted by FIT2. Therefore, we can conclude that the APECs obtained at MRCI(Q)/AV(5 + d)Z level of theory accurately describe the interaction potential of the sulfur dimer molecule in the triplet states analyzed. Furthermore, the novel APECs here reported are strongly recommended to be used as building blocks for larger sulfur-containing systems within a many-body expansion frame.

3.3 Vibrational manifolds

Our next step was to compute the vibrational manifolds for $X^3\Sigma_g^-$ ground and $A'^3\Delta_u$, $A^3\Sigma_u^+$, $B''^3\Pi_u$, and $B^3\Sigma_u^-$ excited triplet electronic states. For this purpose, in this paper we use the LEVEL code (Le Roy 2002), which calculates rovibrational wavefunctions by solving the 1D Schrödinger equation, with the input of our potential energy curves described in the previous section. A good description of PECs and its spectroscopic parameters are essential to perform these calculations since it implies accurate rovibrational levels. Thus, within the adiabatic approximation, the radial Schrödinger equation can be written as

$$\left[\frac{-\hbar^2}{2\mu} \frac{d^2}{dr^2} + \frac{\hbar^2}{2\mu r^2} J(J+1) + V(r) \right] \psi_{v,J}(r) = E_{v,J} \psi_{v,J}(r) \tag{7}$$

where $V(r)$ is the potential interaction, μ is the molecule's reduced mass, and r represents the internuclear separation of the two atoms. On the other hand, $\psi_{v,J}(r)$ and $E_{v,J}$ are the eigenfunctions and eigenvalues, respectively. The vibrational quantum numbers are represented by v , while the rotationals are denoted by J . The present work used the formulation in which, for a given vibrational level, the rotational

Table 3 Vibrational levels G_ν (in cm^{-1}), vibrational term values $G(\nu) = G_\nu - G_0$, classical turning points (in Å) of $D^3\Pi_u$ of the first 10 vibrational states for the sulfur dimer when $J = 0$, based on the RKR method

ν	G_ν	$G(\nu)$	R_{\min}	R_{\max}
0	58914.3	0	1.80574	1.90905
1	59700.0	785.7	1.76901	1.94870
2	60477.8	1563.5	1.74384	1.97682
3	61247.6	2333.3	1.72341	2.00026
4	62009.4	3095.1	1.70571	2.02101
5	62763.2	3848.9	1.68986	2.03996
6	63509.0	4594.7	1.67535	2.05764
7	64246.8	5332.5	1.66185	2.07434
8	64976.6	6062.3	1.64917	2.09029
9	65698.4	6784.1	1.63716	2.10564

sublevel of a determined electronic state can be calculated by the following power series:

$$\begin{aligned}
 E_{\nu,J} = & G(\nu) + B_\nu[J(J+1)] - D_\nu[J(J+1)]^2 \\
 & + H_\nu[J(J+1)]^3 + L_\nu[J(J+1)]^4 \\
 & + M_\nu[J(J+1)]^5 + N_\nu[J(J+1)]^6 \\
 & + O_\nu[J(J+1)]^7
 \end{aligned} \quad (8)$$

where $G(\nu)$ is the vibrational level, B_ν is inertial rotation constant, and D_ν , H_ν , L_ν , M_ν , N_ν , and O_ν are the six centrifugal distortion constants, respectively.

For each electronic state studied, a set of 10 vibrational states were calculated setting $J = 0$, by solving Eq. (8) numerically. These number of vibrational states determined seem to be sufficient to our purposes. Collected in Tables 3 to 9 are the vibrational levels G_ν , vibrational term values $G(\nu)$, classical turning points (R_{\min} and R_{\max}), and rotational constants B_ν . Table 4 also contains theoretical results extracted from Brabson and Volkmar (1973) and Wei et al. (2016) and experimental results from Green and Western (1996). The other six centrifugal distortion constants which compose the rotational structure were discarded since our major interesting was concentrated only in vibrational levels.

In the first stage, analyzing Table 4, there can be observed that the values for $G(\nu)$ and B_ν predicted via FIT2 are in excellent agreement with the corresponding experimental ones (Green and Western 1996). It should be noted that the differences ($G_\nu^{\text{Theo}} - G_\nu^{\text{RKR}}$) between the theoretical values for G_ν (Brabson and Volkmar 1973; Wei et al. 2016) and the RKR data monotonically increase with ν . Meanwhile, FIT1 values differ by 1.38% at $\nu = 0$ level, 0.53% at $\nu = 5$ level, and 0.01% at $\nu = 9$ level. In relation to $G(\nu)$, the deviations between the results provided from FIT2 and

RKR are smaller than 2.0 cm^{-1} for any vibrational quantum number, i.e. $\nu = 0$ to 9, present in this table. However, for FIT1, the maximum deviations are close to 25 cm^{-1} . The differences between the present R_{\min} calculated through FIT1 (FIT2) and the corresponding RKR data are only 0.01557 (0.00666), 0.01501 (0.00664), 0.01489 (0.00663), and 0.01503 (0.00662) Å for $\nu = 0, 1, 2$, and 3 , respectively. Similarly, the deviations between the present R_{\max} and the corresponding RKR data are 0.01646 (0.00657), 0.01609 (0.00657), 0.01580 (0.00659), and 0.01564 (0.00661) Å for $\nu = 0, 1, 2$, and 3 , respectively. For the ground state, we demonstrated that the FIT2 can be useful in computing accurate vibrational energy levels. Rovibrational levels for $S_2(X^3\Sigma_g^-)$ calculated using FIT2 for quantum rotational numbers until 20 are collected in the Supplementary Material (see Table III).

From Table 5, it is verified that FIT1 does not reproduce with high precision the RKR data. In general, the differences $G_\nu^{\text{FIT1}} - G_\nu^{\text{RKR}}$ present a spacing of the order of 500 cm^{-1} . As discussed before, we attributed these limitations to discrepancies found in the spectroscopic parameters regarding the experimental ones. The relative rotational constants $B_\nu^{\text{FIT1}} - B_\nu^{\text{RKR}}$ present deviations of the same order of magnitude (0.03 cm^{-1}) for each vibrational quantum number. Listed in Table 6 one finds our values of G_ν , $G(\nu)$, R_{\min} , R_{\max} and B_ν for the triplet excited state $A^3\Sigma_u^+$. Notably, the results with FIT2 are in close agreement with those estimated via the RKR method. In this case, we believe that in the results provided by FIT2, APEC must be reliable and accurate. To the best of our knowledge, there is no experimental or theoretical work considering the vibrational levels, classical turning points and rotation constants for the excited electronic states $A'^3\Delta_u$ and $A^3\Sigma_u^+$.

The experimental results found in Tables 7 and 8 were taken from Green and Western (1996). For $B^3\Sigma_u^-$ state of S_2 , the agreement between RKR method and those experimental results is good. Yet, FIT2 overestimated the values of G_ν and $G(\nu)$ from the RKR results by ~ 250 and 280 cm^{-1} , respectively, while deviations in R_{\min} and R_{\max} occur typically in the third and second decimal place. Similar observations can be made when comparing FIT2 and the values reported by Green and Western (1996).

3.4 Triplet band systems

At this point, we would like to mention that all our results involving vibronic transitions are calculated according to the restrictions of symmetry and spin conservation contained in the Wigner–Witmer rules (Wigner and Witmer 1928). The same idea has been followed by Sarka et al. (2019). Once that these conditions have been imposed, the next step was to calculate the radiative transition parameters (FC factors

Table 4 Vibrational levels G_ν (in cm^{-1}), vibrational term values $G(\nu) = G_\nu - G_0$, classical turning points (in Å), and rotational constant B_ν (in cm^{-1}) of $X^3\Sigma_g^-$ of the first 10 vibrational states for the sulfur dimer when $J = 0$

ν	Source	G_ν	$G(\nu)$	R_{\min}	R_{\max}	B_ν
0	FIT1	356	0	1.85585	1.96479	0.28896
	FIT2	362	0	1.84694	1.95490	0.29179
	RKR	361	0	1.84028	1.94833	0.29384
	Wei et al. (2016)	363	0	–	–	0.29499
	Brabson and Volkmar (1973)	362	0	1.8373	1.9452	–
	Green and Western (1996)	–	0	–	–	0.29459
1	FIT1	1066	710	1.82041	2.00928	0.28607
	FIT2	1081	719	1.81204	1.99976	0.29022
	RKR	1081	720	1.80540	1.99319	0.29224
	Wei et al. (2016)	1085	722	–	–	0.29340
	Brabson and Volkmar (1973)	1084	722	1.8025	1.9900	–
	Green and Western (1996)	–	720	–	–	0.29299
2	FIT1	1773	1418	1.79756	2.04175	0.28758
	FIT2	1794	1432	1.78930	2.03254	0.28863
	RKR	1794	1433	1.78267	2.02595	0.29065
	Wei et al. (2016)	1801	1438	–	–	0.29180
	Brabson and Volkmar (1973)	1798	1436	1.7797	2.0228	–
	Green and Western (1996)	–	1434	–	–	0.29142
3	FIT1	2478	2122	1.77997	2.06944	0.28444
	FIT2	2501	2139	1.77156	2.06041	0.28705
	RKR	2502	2141	1.76494	2.05380	0.28905
	Wei et al. (2016)	2511	2148	–	–	0.29020
	Brabson and Volkmar (1973)	2505	2143	1.7619	2.0507	–
	Green and Western (1996)	–	2143	–	–	0.28964
4	FIT1	3179	2823	1.76548	2.09444	0.28273
	FIT2	3202	2840	1.75674	2.08547	0.28545
	RKR	3202	2841	1.75010	2.07883	0.28746
	Wei et al. (2016)	3216	2853	–	–	0.28861
	Brabson and Volkmar (1973)	3207	2845	1.7472	2.0756	–
	Green and Western (1996)	–	2846	–	–	0.28837
5	FIT1	3876	3520	1.75309	2.11769	0.28095
	FIT2	3897	3535	1.74388	2.10864	0.28385
	RKR	3897	3536	1.73721	2.10199	0.28586
	Wei et al. (2016)	3915	3552	–	–	0.28701
	Brabson and Volkmar (1973)	3906	3544	1.7344	2.0986	–
	Green and Western (1996)	–	3552	–	–	0.28440
6	FIT1	4567	4211	1.74224	2.13969	0.27913
	FIT2	4586	4224	1.73247	2.13047	0.28225
	RKR	4586	4225	1.72575	2.12380	0.28427
	Wei et al. (2016)	4608	4245	–	–	0.28541
	Brabson and Volkmar (1973)	4595	4233	1.7230	2.1203	–
	Green and Western (1996)	–	4230	–	–	0.28324
7	FIT1	5254	4898	1.73257	2.16077	0.27728
	FIT2	5269	4907	1.72217	2.15127	0.28065
	RKR	5268	4907	1.71538	2.14460	0.28267
	Wei et al. (2016)	5296	4933	–	–	0.28381
	Brabson and Volkmar (1973)	5291	4929	1.7134	2.1400	–
	Green and Western (1996)	–	4920	–	–	0.28324
8	FIT1	5936	5580	1.72384	2.18112	0.27540
	FIT2	5945	5583	1.71276	2.17127	0.27904
	RKR	5944	5583	1.70587	2.16462	0.28108
	Wei et al. (2016)	5978	5615	–	–	0.28221
	Brabson and Volkmar (1973)	5968	5602	1.7032	2.1610	–
	Green and Western (1996)	–	5602	–	–	0.28221
9	FIT1	6612	6256	1.71589	2.20088	0.27352
	FIT2	6616	6254	1.70409	2.19063	0.27743
	RKR	6613	6252	1.69708	2.18402	0.27948

Table 5 Vibrational levels G_v (in cm^{-1}), vibrational term values $G(v) = G_v - G_0$, classical turning points (in \AA), and rotational constant B_v (in cm^{-1}) of $A'^3\Delta_u$ of the first 10 vibrational states for the sulfur dimer when $J = 0$

v	Source	G_v	$G(v)$	R_{\min}	R_{\max}	B_v
0	FIT1	21121	0	2.09912	2.23222	0.22479
	RKR	21600	0	2.08558	2.21732	0.22780
1	FIT1	21593	472	2.05678	2.28845	0.22327
	RKR	22083	483	2.04332	2.27249	0.22640
2	FIT1	22061	940	2.02943	2.32995	0.22173
	RKR	22561	961	2.01584	2.31299	0.22500
3	FIT1	22523	1402	2.00824	2.36556	0.22016
	RKR	23034	1434	1.99440	2.34755	0.22360
4	FIT1	22979	1858	1.99064	2.39785	0.21856
	RKR	23502	1902	1.97649	2.37871	0.22220
5	FIT1	23430	2309	1.97548	2.42799	0.21694
	RKR	23965	2365	1.96095	2.40762	0.22080
6	FIT1	23875	2754	1.96209	2.45664	0.21530
	RKR	24423	2823	1.94714	2.43492	0.21940
7	FIT1	24315	3194	1.95009	2.48421	0.21363
	RKR	24877	3277	1.93465	2.46102	0.21800
8	FIT1	24748	3627	1.93919	2.51100	0.21193
	RKR	25325	3725	1.92323	2.48618	0.21660
9	FIT1	25176	4055	1.92920	2.53722	0.21021
	RKR	25768	4168	1.91267	2.51060	0.21520

and r -centroids). We have followed the methodology described in works of Karthikeyan et al. (2006), Ramachandran et al. (2005), Bagare and Rajamanickam (2004), Urena et al. (2000) and the references therein to accomplish our goal. In short, the relative intensities of a vibrational peaks in an electronically allowed transition are determined by Franck–Condon factors denoted by $q_{v'v''}$ and usually it is expressed as

$$q_{v'v''} = |I_{v'v''}|^2 \quad (9)$$

where $I_{v'v''}$ is the overlap integral defined as

$$I_{v'v''} = \int \psi_{v'} \psi_{v''} dr \quad (10)$$

in this equation, $\psi_{v'}$ and $\psi_{v''}$ represent the normalized vibrational wave functions for the upper and lower states, respectively. On the other hand, the r -centroid ($\bar{r}_{v'v''}$) for a certain vibronic transition, in units of \AA , is defined as

$$\bar{r}_{v'v''} = \frac{\int \psi_{v'} r \psi_{v''} dr}{\int \psi_{v'} \psi_{v''} dr}. \quad (11)$$

The above equation is widely used for calculation of the band strengths of the observed transitions in diatomic molecules. Of course, the accuracy in the calculation of $q_{v'v''}$

Table 6 Vibrational levels G_v (in cm^{-1}), vibrational term values $G(v) = G_v - G_0$, classical turning points (in \AA), and rotational constant B_v (in cm^{-1}) of $A^3\Sigma_u^+$ of the first 10 vibrational states for the sulfur dimer when $J = 0$

v	Source	G_v	$G(v)$	R_{\min}	R_{\max}	B_v
0	FIT1	21743	0	2.10727	2.24143	0.22300
	FIT2	22139	0	2.09541	2.22794	0.22565
1	RKR	22211	0	2.10283	2.23540	0.22410
	FIT1	21593	465	2.06471	2.29829	0.22144
2	FIT2	22617	478	2.05286	2.28332	0.22428
	RKR	22688	477	2.06037	2.29101	0.22270
3	FIT1	22667	924	2.03723	2.34030	0.21987
	FIT2	23089	950	2.02526	2.32395	0.22289
4	RKR	23160	949	2.03277	2.33187	0.22130
	FIT1	23121	1378	2.01595	2.37635	0.21828
5	FIT2	23558	1419	2.00382	2.35866	0.22148
	RKR	23627	1416	2.01125	2.36677	0.21990
6	FIT1	23569	1826	1.99828	2.40903	0.21667
	FIT2	24022	1883	1.98597	2.39001	0.22004
7	RKR	24088	1877	1.99327	2.39825	0.21850
	FIT1	24012	2269	1.98305	2.43953	0.21504
8	FIT2	24481	2342	1.97056	2.41919	0.21857
	RKR	24545	2334	1.97767	2.42748	0.21710
9	FIT1	24450	2707	1.96960	2.46850	0.21339
	FIT2	24935	2796	1.95693	2.44686	0.21708
10	RKR	24996	2785	1.96381	2.45510	0.21570
	FIT1	24881	3138	1.95754	2.49639	0.21172
11	FIT2	25384	3245	1.94469	2.47344	0.21556
	RKR	25443	3232	1.95128	2.48151	0.21430
12	FIT1	25307	3564	1.94658	2.52347	0.21003
	FIT2	25827	3688	1.93355	2.49922	0.21400
13	RKR	25884	3673	1.93981	2.50699	0.21290
	FIT1	25727	3984	1.93654	2.54997	0.20830
14	FIT2	26265	4126	1.92334	2.52441	0.21241
	RKR	26320	4109	1.92922	2.53173	0.21150

and $\bar{r}_{v'v''}$ depends on the choice of suitable potential. Many authors have used the Morse (1929) potential energy interaction. This potential is used within Eq. (7) to solve the radial Schrödinger equation to obtain the Morse wave functions with $J = 0$. From the literature review, it is well documented that this type of potential function can be taken as a fair approximation to realistic wavefunctions, especially for low vibrational levels (Urena et al. 2000). The Morse potential is easily constructed having the spectroscopic parameters.

In this work we adopted the molecular constants used to reproduce RKR potentials to realize calculations of $\psi_{v'}$ and $\psi_{v''}$; see Table 1. Due to reasons already discussed in the case of the $B^3\Sigma_u^- - X^3\Sigma_g^-$ band system, the FC factors,

Table 7 Vibrational levels G_ν (in cm^{-1}), vibrational term values $G(\nu) = G_\nu - G_0$, classical turning points (in Å), and rotational constant B_ν (in cm^{-1}) of $B''^3\Pi_u$ of the first 10 vibrational states for the sulfur dimer when $J = 0$

ν	Source	G_ν	$G(\nu)$	R_{\min}	R_{\max}	B_ν
0	FIT1	31673	0	2.22464	2.38957	0.19796
	RKR	31236	0	2.16752	2.32706	0.20860
	Green and Western (1996)	–	–	–	–	–
1	FIT1	31975	302	2.17459	2.46495	0.19546
	RKR	31562	326	2.12055	2.40007	0.20580
	Green and Western (1996)	–	–	–	–	–
2	FIT1	32266	593	2.14298	2.52415	0.19269
	RKR	31879	643	2.09104	2.45615	0.20300
	Green and Western (1996)	31725	–	–	–	0.20369
3	FIT1	32545	872	2.11903	2.57842	0.18961
	RKR	32188	952	2.06854	2.50578	0.20020
	Green and Western (1996)	32038	–	–	–	0.20169
4	FIT1	32810	1137	2.09965	2.63148	0.18614
	RKR	32487	1251	2.05005	2.55199	0.19740
	Green and Western (1996)	32344	–	–	–	0.19935
5	FIT1	33061	1388	2.08349	2.68564	0.18217
	RKR	32777	1541	2.03419	2.59619	0.19460
	Green and Western (1996)	32640	–	–	–	0.19747
6	FIT1	33294	1621	2.06980	2.74307	0.17752
	RKR	33058	1822	2.02020	2.63916	0.19180
	Green and Western (1996)	32931	–	–	–	0.19450
7	FIT1	33509	1836	2.05820	2.80671	0.17186
	RKR	33330	2094	2.00759	2.68144	0.18900
	Green and Western (1996)	33216	–	–	–	0.19082
8	FIT1	33700	2027	2.04851	2.88184	0.16449
	RKR	33594	2358	1.99605	2.72339	0.18620
	Green and Western (1996)	33485	–	–	–	0.18964
9	FIT1	33858	2185	2.04088	2.98118	0.16368
	RKR	33848	2612	1.98534	2.76528	0.18340
	Green and Western (1996)	33749	–	–	–	0.18651

as well as r -centroids and its corresponding wavenumbers, have been calculated also through the interatomic potential FIT2. Therefore, to do this, the values of spectroscopic parameters contained in Table 2 were used. It should be noted that we restrict the quantum number $\nu' = 6$ for all excited states because we wanted to avoid the predissociation phenomenon involved in the $B^3\Sigma_u^-$ state. Meanwhile for $X^3\Sigma_g^-$ we considered only the ten lowest vibrational levels in all analyses.

Molecular FC factors provide results which can be utilized as a starting point to calculate many other properties of the diatomic systems such as radiative lifetimes and Einstein coefficients. Numerically, the integration in each case was carried out at intervals of 0.001 \AA and the range of transitions analyzed was chosen according to its calculated classical turning points. Tables 10 to 13 show our results collected for vibronic transition probability parameters.

The r -centroid values for (0,0) transition of all the investigated systems are slightly greater than $(r'_e + r''_e)/2$. For $B''^3\Pi_u - X^3\Sigma_g^-$ these quantities differ by 0.0348 \AA , by $0.0688 (0.0551) \text{ \AA}$ for $B^3\Sigma_u^- - X^3\Sigma_g^-$, by 0.0022 and 0.0039 \AA for $C^3\Sigma_u^- - X^3\Sigma_g^-$ and $D^3\Pi_u - X^3\Sigma_g^-$, respectively. These are typical features of very anharmonic potentials. In the case of the C–X system, Anandaraj et al. (1992) reported both FC factors and r -centroids for (0, 0), (0, 2), (0, 3), (0, 4), (0, 5), (0, 6), (1, 0), (1, 3), (1, 4), (1, 5), (3, 6) bands. We included all these results together with ours in Table 12. Our obtained vibronic transition parameters show good agreement with their results with maximum deviation for FC factors less than 8%. In the same table, the r -centroids values computed in this present work are also compared with those accounted by Verma and Mahajan (1988). It is shown satisfactory agreement between results. According to our calculations, the vibronic transitions from the

Table 8 Vibrational levels G_ν (in cm^{-1}), vibrational term values $G(\nu) = G_\nu - G_0$, classical turning points (in Å), and rotational constant B_ν (in cm^{-1}) of $B^3\Sigma_u^-$ of the first 10 vibrational states for the sulfur dimer when $J = 0$

ν	Source	G_ν	$G(\nu)$	R_{\min}	R_{\max}	B_ν
0	FIT1	33012	0	2.15124	2.29584	0.21323
	FIT2	32038	0	2.12241	2.25850	0.21980
	RKR	32051	0	2.10515	2.24494	0.22275
	Green and Western (1996)	31682	0	–	–	0.22420
1	FIT1	33413	401	2.10585	2.35759	0.21156
	FIT2	32492	453	2.07805	2.31445	0.21869
	RKR	32479	428	2.06312	2.30654	0.22045
	Green and Western (1996)	32108	426	–	–	0.22322
2	FIT1	33809	798	2.07674	2.40338	0.20986
	FIT2	32942	904	2.04914	2.35524	0.21754
	RKR	32892	841	2.03676	2.35271	0.21815
	Green and Western (1996)	32530	848	–	–	0.22210
3	FIT1	34199	1187	2.05430	2.44283	0.20814
	FIT2	33388	1350	2.02661	2.38994	0.21635
	RKR	33320	1269	2.01681	2.39270	0.21585
	Green and Western (1996)	32947	1265	–	–	0.21958
4	FIT1	34585	1573	2.03576	2.47875	0.20638
	FIT2	33832	1794	2.00784	2.42122	0.21511
	RKR	33732	1681	2.00060	2.42919	0.21355
	Green and Western (1996)	33354	1672	–	–	0.21983
5	FIT1	34965	1953	2.01985	2.51242	0.20459
	FIT2	34271	2233	1.99161	2.45030	0.21383
	RKR	34138	2087	1.98692	2.46340	0.21125
	Green and Western (1996)	33768	2086	–	–	0.21596
6	FIT1	35340	2328	2.00588	2.54458	0.20277
	FIT2	34706	2668	1.97727	2.47787	0.21250
	RKR	34539	2488	1.97509	2.49601	0.20895
	Green and Western (1996)	34173	2491	–	–	0.21337
7	FIT1	35709	2697	1.99340	2.57569	0.20091
	FIT2	35137	3099	1.96438	2.50436	0.21112
	RKR	34935	2884	1.96469	2.52746	0.20665
	Green and Western (1996)	–	–	–	–	–
8	FIT1	36073	3061	1.98211	2.60608	0.19900
	FIT2	35563	3525	1.95266	2.53010	0.20969
	RKR	35325	3274	1.95544	2.55804	0.20435
	Green and Western (1996)	–	–	–	–	–
9	FIT1	36430	3418	1.97182	2.63599	0.19706
	FIT2	35985	3947	1.94192	2.55530	0.20820
	RKR	35709	3658	1.94713	2.58794	0.20205
	Green and Western (1996)	–	–	–	–	–

lower vibrational levels are stronger than those from higher levels for the two states.

FC factors, r -centroids, and its associated wavenumbers obtained in this work using RKR method for D–X system are listed in Table 13. For comparison purposes, the $q_{\nu'\nu''}$ and $\bar{r}_{\nu'\nu''}$ data from Anandaraj et al. (1992) and Verma and

Mahajan (1988) for (0, 0), (0, 1), (0, 2), (1, 2), (1, 3), and (2, 3) bands are also reported. Again, high concordance between the results can be seen. Very small transition probabilities are estimated above the ($\nu' = 0$, $\nu'' = 5$) band. The small values of the FC factors in this table may be indicating that absorption or fluorescence transitions only with dif-

Table 9 Vibrational levels G_v (in cm^{-1}), vibrational term values $G(v) = G_v - G_0$, classical turning points (in Å), and rotational constant B_v (in cm^{-1}) of $C^3\Sigma_u^-$ of the first 10 vibrational states for the sulfur dimer when $J = 0$

v	G_v	$G(v)$	R_{\min}	R_{\max}	B_v
0	55994	0	1.76135	1.86239	0.32125
1	56871	877	1.72794	1.90354	0.31995
2	57632	1638	1.70590	1.93337	0.31865
3	58441	2447	1.68851	1.95859	0.31735
4	59244	3250	1.67385	1.98115	0.31605
5	60040	4046	1.66101	2.00193	0.31475
6	60829	4835	1.64951	2.02143	0.31345
7	61611	5617	1.63904	2.03995	0.31215
8	62387	6393	1.62939	2.05772	0.31085
9	63156	7162	1.62042	2.07486	0.30955

ficuity occur. As a consequence, the $D^3\Pi_u-X^3\Sigma_g^-$ system exhibits few vibronic transitions. For this reason, it is expected that they are very difficult to measure; however, to verify this evidence more experimental results are necessary. The FC factors calculated for the $\Delta v = v' - v'' = 0$ bands are most intense.

In Tables V and VI of the Supplementary Material can be found comparisons between our predicted values for wavelengths linked with C–X and D–X band systems and the available theoretical and experimental ones (Anandaraj et al. 1992; Tanaka and Ogawa 1962). For C–X and D–X systems, as r'_e is smaller than r''_e and $\bar{r}_{v'v''}$ decrease with the increase of wavelength, it is expected that these bands de-grade for blue. The similar assumption is given by Anandaraj et al. (1992). A major predominant contribution of transition probabilities is given by the C–X to D–X system, although q_{00} (0.8047) for D–X is greater than q_{00} (0.2919) for the C–X system.

Experimentally, the FC factors have been estimated from measurements of the intensity by Anderson et al. (1979) covering a range of $v' = 0-9$ to $v'' = 0-33$ for the $B^3\Sigma_u^- - X^3\Sigma_g^-$ system. On the other hand, using Morse wave functions (Herman and Felenbok 1963) determined the theoretical FC factors for the same transition in the range of $v' = 0-12$ to $v'' = 0-12$. Smith and Liszt (1971) collected both FC factors and *r*-centroids using for such RKR methodology. There, the vibrational quantum numbers were chosen in the range of $v' = 0-26$ to $v'' = 0-2$ and $v' = 0-2$ to $v'' = 0-26$. These results are contained in Tables 7 and 8 from Smith and Liszt (1971). Tabulated in Table 11 are

Table 10 Franck–Condon factors, *r*-centroids (in Å) and wavenumbers (in cm^{-1}) for $B''^3\Pi_u - X^3\Sigma_g^-$ band system

		$v'' = 0$	$v'' = 1$	$v'' = 2$	$v'' = 3$	$v'' = 4$	$v'' = 5$	$v'' = 6$	$v'' = 7$	$v'' = 8$	$v'' = 9$
$v' = 0$	(a)	< 0.0001	< 0.0001	< 0.0001	0.0001	0.0006	0.0020	0.0055	0.0127	0.0251	0.0434
	(b)	2.0388	2.0543	2.0699	2.0856	2.1014	2.1173	2.1333	2.1495	2.1658	2.1822
	(c)	30875	30155	29442	28734	28034	27339	26650	25968	25292	25223
$v' = 1$	(a)	< 0.0001	< 0.0001	0.0002	0.0010	0.0038	0.0106	0.0237	0.0435	0.0657	0.0819
	(b)	2.0317	2.0470	2.0625	2.0781	2.0938	2.1096	2.1254	2.1414	2.1576	2.1738
	(c)	31201	30481	29768	29060	28360	27665	26976	26294	25618	24949
$v' = 2$	(a)	< 0.0001	0.0001	0.0009	0.0039	0.0120	0.0278	0.0496	0.0684	0.0717	0.0534
	(b)	2.0247	2.0400	2.0553	2.0708	2.0864	2.1020	2.1177	2.1336	2.1495	2.1654
	(c)	31151	30798	30085	29377	28677	27982	27293	26611	25935	25266
$v' = 3$	(a)	< 0.0001	0.0005	0.0027	0.0100	0.0258	0.0480	0.0647	0.0610	0.0350	0.0068
	(b)	2.0179	2.0331	2.0484	2.0637	2.0791	2.0946	2.1102	2.1258	2.1414	2.1560
	(c)	31827	31107	30394	29686	28986	28291	27602	26920	26244	25575
$v' = 4$	(a)	0.0001	0.0012	0.0063	0.0199	0.0417	0.0598	0.0560	0.0285	0.0028	0.0060
	(b)	2.0114	2.0264	2.0416	2.0568	2.0721	2.0875	2.1028	2.1181	2.1315	2.1527
	(c)	32126	31406	30693	29985	29285	28590	27901	27219	26543	25874
$v' = 5$	(a)	0.0003	0.0027	0.0121	0.0319	0.0533	0.0554	0.0301	0.0030	0.0064	0.0315
	(b)	2.0049	2.0199	2.0350	2.0501	2.0652	2.0804	2.0955	2.1088	2.1294	2.1438
	(c)	32416	31696	30983	30275	29575	28880	28191	27509	26833	26164
$v' = 6$	(a)	0.0006	0.0052	0.0199	0.0432	0.0552	0.0372	0.0067	0.0035	0.0276	0.0350
	(b)	1.9987	2.0136	2.0285	2.0435	2.0586	2.0735	2.0876	2.1075	2.1210	2.1360
	(c)	32697	31977	31264	30556	29856	29161	28472	27790	27114	26445

Note: (a) $q_{v'v''}$, (b) $\bar{r}_{v'v''}$, (c) wavenumber

Table 11 Franck–Condon factors, r -centroids (in Å) and wavenumbers (in cm^{-1}) for $B^3\Sigma_u^- - X^3\Sigma_g^-$ band system

		$v'' = 0$	$v'' = 1$	$v'' = 2$	$v'' = 3$	$v'' = 4$	$v'' = 5$	$v'' = 6$	$v'' = 7$	$v'' = 8$	$v'' = 9$
$v' = 0$	(a)	(i) 0.0031	0.0581	0.0021	0.0277	0.0279	0.0008	0.0319	0.0114	0.0083	0.0306
		(ii) 0.0051	0.0535	0.0292	0.0007	0.0316	0.0146	0.0057	0.0300	0.0026	0.0181
	(b)	(i) 2.0997	1.9474	1.9578	1.9779	1.9911	2.0167	2.0227	2.0354	2.0567	2.0690
		(ii) 2.0981	1.9742	1.9851	2.0137	2.0129	2.0227	2.0454	2.0532	2.0569	2.0857
	(c)	(i) 31690	30970	30257	29549	28849	28154	27465	26783	26107	25438
		(ii) 31676	30957	30244	29537	28836	28141	27452	26769	26093	25422
$v' = 1$	(a)	(i) 0.0309	0.0022	0.0104	0.0314	0.0654	0.0981	0.1060	0.0782	0.0318	0.0017
		(ii) 0.0374	0.0010	0.0058	0.0212	0.0522	0.0904	0.1104	0.0897	0.0393	0.0023
	(b)	(i) 2.1912	2.0208	2.0374	2.0542	2.0712	2.0884	2.1058	2.1233	2.1407	2.1532
		(ii) 2.2099	2.0401	2.0554	2.0711	2.0873	2.1039	2.1210	2.1384	2.1556	2.1651
	(c)	(i) 32118	31398	30685	29977	29277	28585	27893	27211	26535	25866
		(ii) 32130	31411	30698	29991	29290	28595	27906	27223	26547	25876
$v' = 2$	(a)	(i) 0.0615	0.0076	0.0289	0.0651	0.0926	0.0807	0.0343	0.0009	0.0169	0.0586
		(ii) 0.0677	0.0034	0.0167	0.0470	0.0829	0.0901	0.0512	0.0057	0.0106	0.0576
	(b)	(i) 2.1771	2.0109	2.0272	2.0438	2.0605	2.0772	2.0938	2.1030	2.1328	2.1495
		(ii) 2.1935	2.0306	2.0454	2.0607	2.0763	2.0922	2.1080	2.1198	2.1510	2.1658
	(c)	(i) 32531	31811	31098	30390	29690	28995	28306	27624	26948	26279
		(ii) 32580	31861	31148	30441	29740	29045	28356	27673	26997	26326
$v' = 3$	(a)	(i) 0.0021	0.0183	0.0537	0.0850	0.0715	0.0217	0.0008	0.0340	0.0618	0.0373
		(ii) 0.0009	0.0085	0.0331	0.0697	0.0812	0.0427	0.0017	0.0197	0.0605	0.0471
	(b)	(i) 2.1743	2.0013	2.0174	2.0336	2.0499	2.0657	2.0945	2.1030	2.1196	2.1364
		(ii) 2.2104	2.0214	2.0359	2.0506	2.0656	2.0803	2.0857	2.1192	2.1340	2.1500
	(c)	(i) 32959	32239	31526	30818	30118	29423	28734	28052	27376	26707
		(ii) 33026	32307	31594	30887	30186	29491	28802	28119	27443	26772
$v' = 4$	(a)	(i) 0.0524	0.0341	0.0739	0.0747	0.0255	0.0007	0.0353	0.0541	0.0188	0.0015
		(ii) 0.0506	0.0166	0.0508	0.0763	0.0500	0.0042	0.0156	0.0536	0.0338	0.0001
	(b)	(i) 2.1542	1.9918	2.0077	2.0236	2.0391	2.0673	2.0751	2.0911	2.1068	2.1355
		(ii) 2.1687	2.0126	2.0267	2.0409	2.0550	2.0644	2.0919	2.1053	2.1200	2.0799
	(c)	(i) 33371	32651	31938	31230	30530	29835	29146	28464	27788	27118
		(ii) 33470	32751	32038	31331	30630	29935	29246	28563	27887	27216
$v' = 5$	(a)	(i) 0.0171	0.0518	0.0790	0.0420	0.0004	0.0268	0.0506	0.0154	0.0039	0.0401
		(ii) 0.0286	0.0271	0.0636	0.0633	0.0155	0.0053	0.0443	0.0346	0.0002	0.0276
	(b)	(i) 2.1402	1.9827	1.9983	2.0137	2.0182	2.0485	2.0640	2.0789	2.1035	2.1165
		(ii) 2.1514	2.0042	2.0178	2.0315	2.0437	2.0689	2.0791	2.0928	2.0714	2.1310
	(c)	(i) 33777	33057	32344	31636	30936	30241	29552	28870	28194	27525
		(ii) 33909	33190	32477	31770	31069	30374	29685	29002	28326	27655
$v' = 6$	(a)	(i) 0.0069	0.0668	0.0660	0.0108	0.0114	0.0477	0.0216	0.0019	0.0366	0.0315
		(ii) 0.0003	0.0384	0.0673	0.0386	0.0002	0.0281	0.0413	0.0036	0.0182	0.0418
	(b)	(i) 2.1353	1.9737	1.9890	2.0032	2.0235	2.0379	2.0528	2.0784	2.0888	2.1043
		(ii) 2.1824	1.9961	2.0093	2.0221	2.0050	2.0550	2.0678	2.0751	2.1045	2.1174
	(c)	(i) 34178	33458	32745	32037	31337	30642	29953	29271	28595	27926
		(ii) 34344	33625	32912	32205	31504	30809	30120	29437	28761	28090

Note: (a) $q_{v'v''}$, (b) $\bar{r}_{v'v''}$, (c) wavenumber

(i) RKR method, (ii) FIT2

Table 12 Franck–Condon factors, *r*-centroids (in Å) and wavenumbers (in cm⁻¹) for C³Σ_u⁻ – X³Σ_g⁻ band system

		<i>v</i> ' = 0	<i>v</i> ' = 1	<i>v</i> ' = 2	<i>v</i> ' = 3	<i>v</i> ' = 4	<i>v</i> ' = 5	<i>v</i> ' = 6	<i>v</i> ' = 7	<i>v</i> ' = 8	<i>v</i> ' = 9
<i>v</i> ' = 0	(a)	(i) 0.2919	0.3335	0.2137	0.1016	0.0400	0.0139	0.0044	0.0013	0.0004	0.0001
		(ii) 0.317	–	0.204	0.091	0.034	0.011	0.003	–	–	–
	(b)	(i) 1.8531	1.8220	1.7928	1.7652	1.7391	1.7142	1.6902	1.6672	1.6450	1.6234
		(ii) 1.852	–	1.789	1.761	1.733	1.707	1.682	–	–	–
		(iii) 1.8520	–	1.7948	1.7705	1.7484	1.7282	–	–	–	–
	(c)	55633	54913	54200	53492	52792	52097	51408	50726	50050	49381
<i>v</i> ' = 1	(a)	(i) 0.3863	0.0153	0.0806	0.1866	0.1641	0.0962	0.0446	0.0177	0.0063	0.0021
		(ii) 0.390	–	–	0.199	0.159	0.086	–	–	–	–
	(b)	(i) 1.8887	1.8464	1.8299	1.7986	1.7706	1.7442	1.7191	1.6952	1.6722	1.6499
		(ii) 1.889	–	–	1.795	1.766	1.739	–	–	–	–
		(iii) 1.8915	–	–	1.7989	1.7745	1.7522	–	–	–	–
	(c)	56510	55790	55077	54369	53669	52974	52285	51603	50927	50258
<i>v</i> ' = 2	(a)	(i) 0.2260	0.1372	0.1432	0.0004	0.0729	0.1447	0.1297	0.0803	0.0397	0.0169
	(b)	(i) 1.9265	1.8965	1.8592	1.7626	1.8059	1.7762	1.7494	1.7242	1.7002	1.6771
	(c)	57261	56541	55828	55120	54420	53725	53036	52354	51678	51009
<i>v</i> ' = 3	(a)	(i) 0.0769	0.2761	0.0053	0.1542	0.0515	0.0059	0.0810	0.1239	0.1047	0.0648
		(ii) –	–	–	–	–	–	0.102	–	–	–
	(b)	(i) 1.9671	1.9326	1.9234	1.8663	1.8302	1.8239	1.7826	1.7549	1.7294	1.7052
		(ii) –	–	–	–	–	–	1.778	–	–	–
	(c)	58080	57360	56647	55939	55239	54544	53855	53173	52497	51828
	<i>v</i> ' = 4	(a)	(i) 0.0769	0.2761	0.0053	0.1542	0.0515	0.0059	0.0810	0.1239	0.1047
(b)		(i) 1.9671	1.9326	1.9234	1.8663	1.8302	1.8239	1.7826	1.7549	1.7294	1.7052
(c)		58883	58163	57450	56742	56042	55347	54658	53976	53300	52631
<i>v</i> ' = 5	(a)	(i) 0.0168	0.1711	0.1912	0.0254	0.0801	0.1047	0.0087	0.0240	0.0882	0.1080
	(b)	(i) 2.0112	1.9728	1.9395	1.8907	1.8744	1.8381	1.7970	1.7918	1.7608	1.7347
	(c)	59679	58959	58246	57538	56838	56143	55454	54772	54096	53427
<i>v</i> ' = 6	(a)	(i) 0.0003	0.0108	0.1070	0.2296	0.0138	0.1252	0.0008	0.0721	0.0782	0.0096
	(b)	(i) 2.1142	2.0653	2.0224	1.9850	1.9679	1.9102	1.8073	1.8525	1.8184	1.7806
	(c)	60468	59748	59035	58327	57627	56932	56243	55561	54885	54216

Note: (a) *q*_{*v*'*v*''}, (b) $\bar{r}_{v'v''}$, (c) wavenumber

(i) RKR method, (ii) Anandaraj et al. (1992), (iii) Verma and Mahajan (1988)

our predicted values for this transition. As previously mentioned, specially for this case RKR and FIT2 PECs have been used.

According to our results for the B³Σ_u⁻–X³Σ_g⁻ transition the FC factors *q*_{*v*'*v*''} are 0.0031 and 0.0051 for RKR and FIT2 PECs, respectively. In both cases, the transitions with Δ*v* = –1, (0, 1), (1, 2), and (2, 3), have larger Franck–Condon factors than Δ*v* = 0. As *r*'_{*e*} > *r*''_{*e*} and $\bar{r}_{v'v''}$ value increases with the increase of wavelength, it is expected that these bands degrade towards the red region. This assumption agrees with experimental results from Smith and Hopkins (1981). There, the (3, 3) band was observed at 324.47 nm. The corresponding values determined here point to dif-

ferences of 0.02 (RKR) and 0.71 (FIT2) nm from this measurement.

From our calculations, the B³Π_u–X³Σ_g⁻ values show weak transitions associated to lower vibrational levels, such as (0, 0), (0, 1), (0, 2), (0, 3), (0, 4), (1, 0), (1, 1), (1, 2), (2, 0), (2, 1), (2, 2), (3, 0), (3, 1), and (4, 0); see Table 10. We observed that the FC factors increase slightly as the vibrational quantum numbers increase. As *r*'_{*e*} > *r*''_{*e*} and the $\bar{r}_{v'v''}$ value increases with the decrease of wavenumbers, it is the expected that these bands degrade towards the red region. In order to better visualize these results, we plot the results of Tables 10 to 13 in Fig. 3.

The B³Σ_u⁻–X³Σ_g⁻ transitions were observed in the interval of 280 and 320 nm in the spectra of Comet Hyakutake

Table 13 Franck–Condon factors, r -centroids (in Å) and wavenumbers (in cm^{-1}) for $D^3\Pi_u - X^3\Sigma_g^-$ band system

		$v'' = 0$	$v'' = 1$	$v'' = 2$	$v'' = 3$	$v'' = 4$	$v'' = 5$	$v'' = 6$	$v'' = 7$	$v'' = 8$	$v'' = 9$	
$v' = 0$	(a)	(i) 0.8047	0.1724	0.0216	0.0019	0.0001	< 0.0001	–	–	–	–	
		(ii) 0.8110	0.1680	0.020	–	–	–	–	–	–	–	
		(iii) 0.5423	0.3154	0.1121	–	–	–	–	–	–	–	
	(b)	(i) 1.8748	1.7982	1.7242	1.6417	1.5303	–	–	–	–	–	
		(ii) 1.875	1.797	1.721	–	–	–	–	–	–	–	
		(iii) 1.8761	1.8180	1.7790	–	–	–	–	–	–	–	
	(c)	58553	57833	57120	56412	–	–	–	–	–	–	
	$v' = 1$	(a)	(i) 0.1790	0.4983	0.2636	0.0528	0.0065	0.0005	< 0.0001	–	–	–
			(ii) –	–	0.2580	0.0490	–	–	–	–	–	–
(iii) –			–	0.2713	0.1879	–	–	–	–	–	–	
(b)		(i) 1.9586	1.8826	1.8040	1.7302	1.6490	1.5412	–	–	–	–	
		(ii) –	–	1.8030	1.7270	–	–	–	–	–	–	
		(iii) –	–	1.8226	1.7827	–	–	–	–	–	–	
(c)		59339	58619	57906	57198	–	–	–	–	–	–	
$v' = 2$		(a)	(i) 0.0164	0.2861	0.2955	0.3018	0.0860	0.0136	0.0013	0.0001	< 0.0001	–
			(ii) –	–	–	0.2970	–	–	–	–	–	–
	(iii) –		–	–	0.1413	–	–	–	–	–	–	
	(b)	(i) 2.0445	1.9672	1.8907	1.8097	1.7359	1.6558	1.5513	1.3578	–	–	
		(ii) –	–	–	1.8090	–	–	–	–	–	–	
		(iii) –	–	–	1.8273	–	–	–	–	–	–	
	(c)	60116	59396	58683	57975	–	–	–	–	–	–	
	$v' = 3$	(a)	(i) 0.0007	0.0417	0.3442	0.1651	0.3065	0.1168	0.0229	0.0027	0.0002	–
		(b)	(i) 2.1598	2.0536	1.9761	1.8996	1.8151	1.7414	1.6623	1.5607	1.3790	–
(c)		60116	59396	58683	57975	–	–	–	–	–	–	
$v' = 4$	(a)	(i) < 0.0001	0.0022	0.0710	0.3699	0.0844	0.2915	0.1429	0.0338	0.0047	0.0004	
	(b)	(i) –	2.1722	2.0628	1.9853	1.9100	1.8203	1.7467	1.6685	1.5695	1.3980	
	(c)	60116	59396	58683	57975	–	–	–	–	–	–	
$v' = 5$	(a)	(i) –	–	0.0047	0.1014	0.3746	0.0373	0.2658	0.1634	0.0456	0.0074	
	(b)	(i) –	–	2.1849	2.0721	1.9948	1.9236	1.8253	1.7517	1.6744	1.5778	
	(c)	60116	59396	58683	57975	–	–	–	–	–	–	

Note: (a) $q_{v'v''}$, (b) $\bar{r}_{v'v''}$, (c) wavenumber

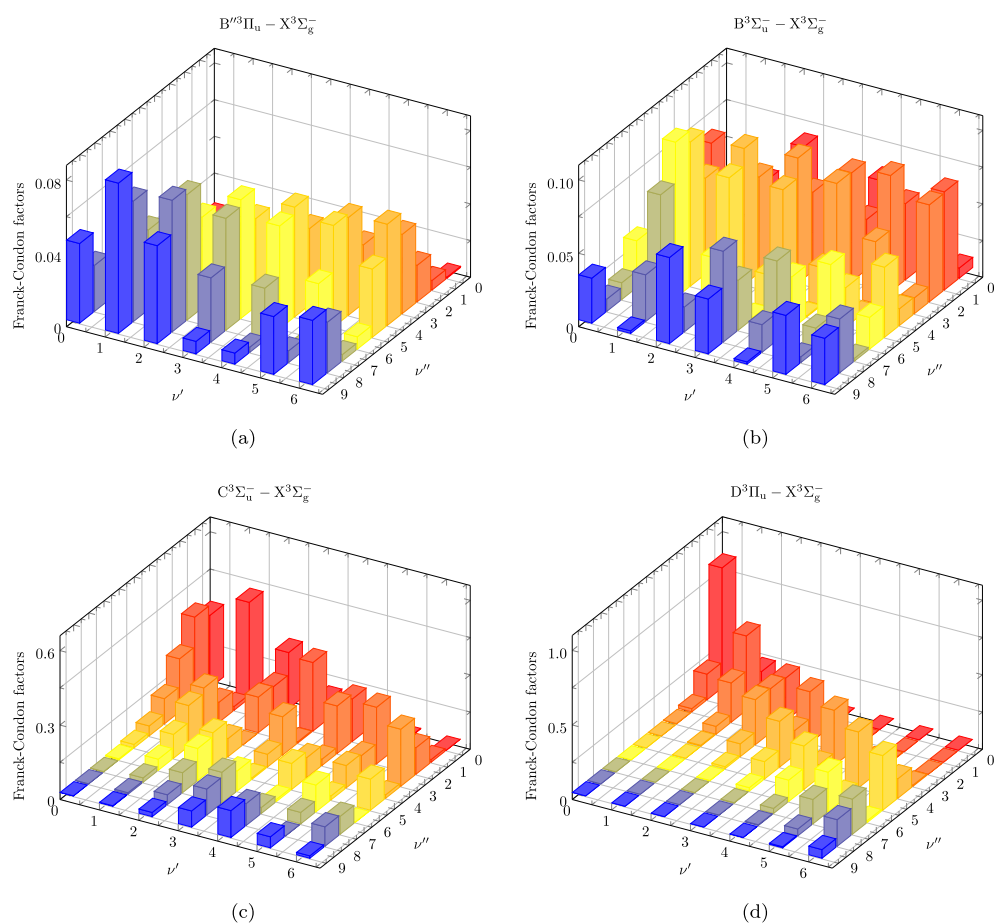
(i) RKR method, (ii) Anandaraj et al. (1992), (iii) Verma and Mahajan (1988)

(C/1996 B2) (Laffont et al. 1998). The model of Reylé and Boice (2003) based on the observations from Kitt Peak Observatory for the same comet predict that the most intense bands are (0, 6), (1, 3), (1, 4), (1, 5), (1, 6), (2, 3), (2, 4), (2, 5), (3, 2), (3, 3), (3, 4), (4, 2), and (5, 2) in the wavelength range of 310 up to 350 nm. A comparison of our computed wavelengths and those from Laffont et al. (1998) and Reylé and Boice (2003) is presented in the Supplementary Material (Table IV). We verify a fair accord with previous results.

Finally, in Fig. 4 we show the absorption (right panels) and fluorescence (left panels) spectra of the $B^3\Sigma_u^- - X^3\Sigma_g^-$ vibronic transition attained in this work. It can be seen these

transitions were investigated separately. Together with our results (RKR and FIT2) are the theoretical (Herman and Felenbok 1963; Smith and Liszt 1971; Meyer and Crosley 1973) and experimental (Anderson et al. 1979) ones. Seemingly, our results are in good agreement with previously reported in the literature. However, we find a discordance between results to $q_{0v''}$ and $q_{v'0}$. We believe that it could be related with a possible non-vertical electronic transitions effects since r'_e is greater than r''_e . Another interpretation for this disagreement is attributing it to strong spin–orbit mixing between the $B''^3\Pi_u$ and $B^3\Sigma_u^-$ states, as pointed out earlier by Green and Western (1996).

Fig. 3 The calculated Franck–Condon factors of triplet–triplet vibronic transitions using RKR method for the lowest vibrational levels



4 Conclusions and final remarks

In the present paper, initially the PECs of the five electronic states $X^3\Sigma_g^-$, $A'^3\Delta_u$, $A^3\Sigma_u^+$, $B''^3\Pi_u$, and $B^3\Sigma_u^-$ of the S_2 molecule have been investigated using the MRCI-F12 approach in combination with the AVQZ basis set of Dunning and co-workers. For such analyses ab initio electronic energies were extracted from Sarka et al. (2019). Both the EHF and the dynamical correlation parts of the calculated energies have been modeled analytically using forms from the realistic EHFACE model. In this first stage, we call these fits “FIT1”.

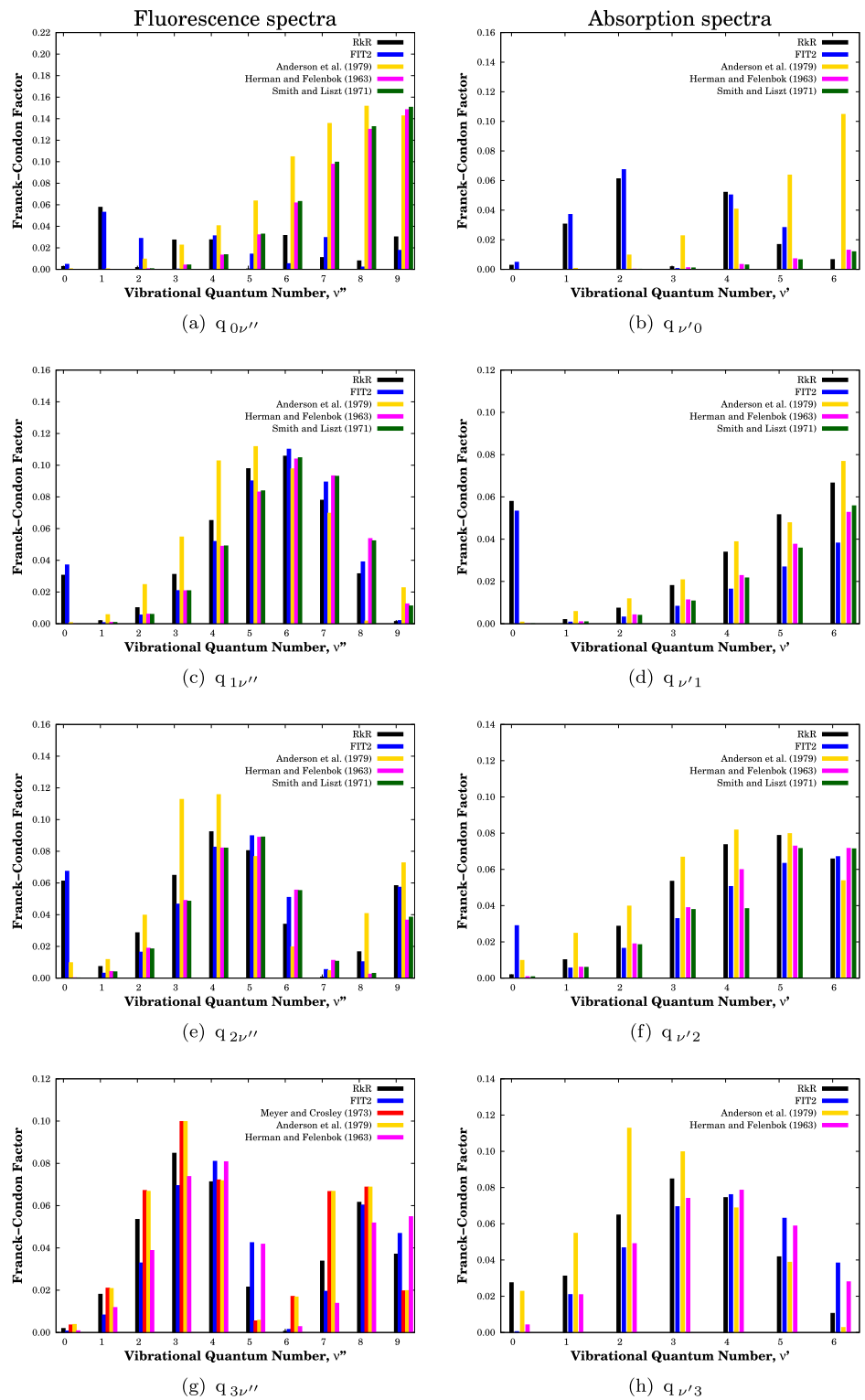
The molecular properties calculated from FIT1 showed some discrepancies in relation not only to the current-generation *state-of-the-art ab initio* calculations but also the experimental ones. Consequently, we proposed to perform novel ab initio calculations at the MRCI(Q)/AV(5 + d)Z level of the theory to improve these relative differences. In this second stage only $X^3\Sigma_g^-$, $A^3\Sigma_u^+$, and $B^3\Sigma_u^-$ of the S_2 molecule have been tested (FIT2). Thereby, the effects on the PECs by tight d functions are discussed in detail. The new set of spectroscopic parameters determined from FIT2 reproduce well the available experimental data. RKR potentials are also included.

In the next stage, the complete set of vibrational states have been carried out using the LEVEL program. For each vibrational state, we computed its corresponding classical turning points and inertial rotation constants. Additionally, the vibrational levels and turning points of the two Rydberg states $C^3\Sigma_u^-$ and $D^3\Pi_u$ were computed only within the RKR method.

The vibronic transition parameters such as the Franck–Condon factors and r -centroids for the bands of the $B''^3\Pi_u - X^3\Sigma_g^-$, $B^3\Sigma_u^- - X^3\Sigma_g^-$, $C^3\Sigma_u^- - X^3\Sigma_g^-$, and $D^3\Pi_u - X^3\Sigma_g^-$ systems have been calculated. These values reported are in good agreement with the available information. It is shown also in the Supplementary Material how our wavelengths related to $B^3\Sigma_u^- - X^3\Sigma_g^-$ are compared to those observed in Comet Hyakutake (Reylé and Boice 2003; Laffont et al. 1998).

In conclusion, based on all the discussions above, we believe that these results reveal valuable information which can help to make predictions for the triplet–triplet vibronic transitions of sulfur dimer; besides, this could serve as a great help in the observations and the treatment of the observational data of reactions involving S-compounds in the interstellar medium.

Fig. 4 The fluorescence spectra (left) and absorption spectra (right) of $B^3\Sigma_u^- - X^3\Sigma_g^-$ band system. The yellow columns represent the experimental results from Anderson et al. (1979). The theoretical results obtained by Herman and Felenbok (1963) (magenta), Smith and Liszt (1971) (green), and Meyer and Crosley (1973) (red) are included for comparisons



Acknowledgements This study was financed by the Coordenação de Aperfeiçoamento de Pessoal de Nível Superior (CAPES)—Finance Code 001.

Publisher’s Note Springer Nature remains neutral with regard to jurisdictional claims in published maps and institutional affiliations.

References

Ahearn, M.F., Schleicher, D.G., Feldman, P.D.: *Astrophys. J.* **274**, L99 (1983)
 Anandaraj, R., Sankaralingam, T., Asokarajan, R., Rajamanickam, N.: *Bull. Astron. Soc. India* **20**, 279 (1992)

- Anderson, W.R., Crosley, D.R., Allen, J.E. Jr.: *J. Chem. Phys.* **71**, 821 (1979) and the references therein
- Anderson, D.E., Bergin, E.A., Maret, S., Wakelam, V.: *Astrophys. J.* **779**, 141 (2013)
- Araújo, J.P., Alves, M.D., da Silva, R.S., Ballester, M.Y.: *J. Mol. Model.* **25**, 198 (2019)
- Ashman, S., et al.: *J. Chem. Phys.* **136**, 114313 (2012)
- Bagare, S.P., Rajamanickam, N.: *Astrophys. Space Sci.* **289**, 9 (2004)
- Ballester, M.Y., Varandas, A.J.C.: *Phys. Chem. Chem. Phys.* **7**, 2305 (2005)
- Barrow, R.F., Du Parcq, R.P.: *J. Phys. B, At. Mol. Phys.* **1**, 283 (1968)
- Barrow, R.F., Du Parcq, R.P., Ricks, J.M.: *J. Phys. B, At. Mol. Phys.* **2**, 413 (1969)
- Bell, R.D., Wilson, A.K.: *Chem. Phys. Lett.* **394**, 105 (2004)
- Brabson, G.D., Volkmar, R.L.: *J. Chem. Phys.* **58**, 3209 (1973)
- Carleer, M., Colin, R.: *J. Phys. B, At. Mol. Phys.* **3**, 1715 (1970)
- da Silva, R.S., Ballester, M.Y.: *J. Chem. Phys.* **149**, 144309 (2018)
- da Silva, M.L., Guerra, V., Loureiro, J., Sá, P.A.: *Chem. Phys.* **348**, 187 (2008)
- Druard, C., Wakelam, V.: *Mon. Not. R. Astron. Soc.* **426**, 354 (2012)
- Dunham, J.L.: *Phys. Rev.* **41**, 721 (1932)
- Dunning, T.H. Jr., Peterson, K.A., Wilson, A.K.: *J. Chem. Phys.* **114**, 9244 (2001)
- Engelke, F., Zare, R.N.: *Chem. Phys.* **19**, 327 (1977)
- Feldman, P.D., Weaver, H.A., A'Hearn, M.F., Festou, M.C., McPhate, J.B., Tozzi, G.P.: *Bull. Am. Astron. Soc.* **31**, 1127 (1999)
- Gerasimova, V.I., Rybaltovskii, A.O., Chernov, P.V., Zimmerer, G.: *Glass Phys. Chem.* **28**, 59 (2002)
- Green, M.E., Western, C.M.: *J. Chem. Phys.* **104**, 848 (1996)
- Herman, L., Felenbok, P.: *J. Quant. Spectrosc. Radiat. Transf.* **3**, 247 (1963)
- Huber, K.P., Herzberg, G.: *Molecular Spectra and Molecular Structure IV, Constants of Diatomic Molecules*. Van Nostrand, New York (1979)
- Jiménez-Escobar, A., Caro, G.M.: *Astron. Astrophys.* **536**, A91 (2011)
- Jiménez-Escobar, A., et al.: *Astrophys. J. Lett.* **751**, L40 (2012)
- Karthikeyan, B., Raja, V., Rajamanickam, N., Bagare, S.P.: *Astrophys. Space Sci.* **306**, 231 (2006)
- Klein, O.: *Z. Phys.* **76**, 226 (1932)
- Laffont, C., et al.: *Geophys. Res. Lett.* **25**, 2749 (1998)
- Langhoff, S.R., Davidson, E.R.: *Int. J. Quant. Chem.* **8**, 61 (1974)
- Le Roy, R.J.: *LEVEL 7.5: A Computer Program for Solving the Radial Schrödinger Equation for Bound and Quasibound Levels*. University of Waterloo, Waterloo (2002)
- Le Roy, R.J.: *J. Quant. Spectrosc. Radiat. Transf.* **186**, 158 (2017)
- Lee, Y.P., Pimentel, G.C.: *J. Chem. Phys.* **70**, 692 (1979)
- Lucas, R., Guélin, M., Kahane, C., Audinos, P., Cernicharo, J.: *Astrophys. Space Sci.* **224**, 293 (1995)
- Maurellis, A.N., Cravens, T.E.: *Icarus* **154**, 350–371 (2001)
- Meyer, K.A., Crosley, D.R.: *J. Chem. Phys.* **59**, 3153 (1973)
- Morse, P.M.: *Phys. Rev.* **34**, 57 (1929)
- Narasimham, N.A., Apparao, K.V.S.R., Balasubramanian, T.K.: *J. Mol. Spectrosc.* **59**, 244 (1976a)
- Narasimham, N.A., Sethuraman, V., Apparao, K.V.S.R.: *J. Mol. Spectrosc.* **59**, 142 (1976b)
- Noll, K.S., et al.: *Science* **267**, 1307 (1995)
- Patinõ, P., Barrow, R.F.: *J. Chem. Soc. Faraday Trans.* **278**, 1271 (1982)
- Pradhan, A.D., Partridge, H.: *Chem. Phys. Lett.* **255**, 163 (1996)
- Qin, Z., et al.: *J. Chem. Phys.* **150**, 044302 (2019)
- Ramachandran, P.S., Rajamanickam, N., Bagare, S.P., Kumar, B.C.: *Astrophys. Space Sci.* **295**, 443 (2005)
- Rees, A.L.G.: *Proc. Phys. Soc. Lond.* **59**, 998 (1947)
- Reylé, C., Boice, D.C.: *Astrophys. J.* **578**, 464 (2003)
- Rydberg, R.: *Z. Phys.* **73**, 376 (1931)
- Rydberg, R.: *Z. Phys.* **80**, 514 (1933)
- Sarka, K., Danielache, S.O., Kondorskiy, A., Nanbu, S.: *Chem. Phys.* **516**, 108 (2019)
- Saxena, P.P., Misra, A.: *Mon. Not. R. Astron. Soc.* **272**, 89 (1995)
- Saxena, P.P., Singh, M., Bhatnagar, S.: *Bull. Astron. Soc. India* **31**, 75 (2003)
- Smith, A.L., Hopkins, J.B.: *J. Chem. Phys.* **75**, 947 (1981)
- Smith, W.H., Liszt, H.S.: *J. Quant. Spectrosc. Radiat. Transf.* **11**, 45 (1971)
- Song, Y.Z., Varandas, A.J.C.: *J. Phys. Chem. A* **115**, 5274 (2011)
- Song, Y.Z., et al.: *Mol. Phys.* **116**, 129 (2018)
- Spencer, J.R., et al.: *Science* **288**, 1208 (2000)
- Tanaka, Y., Ogawa, M.: *J. Chem. Phys.* **36**, 726 (1962)
- Urena, F.P., Gomez, M.F., Gonzalez, J.L., Rajamanickam, N.: *Astrophys. Space Sci.* **272**, 345 (2000)
- van der Tak, F.F., Boonman, A.M.S., Braakman, R., van Dishoeck, E.F.: *Astron. Astrophys.* **412**, 133 (2003)
- Varandas, A.J.C., Silva, J.D.: *J. Chem. Soc. Faraday Trans.* **88**, 941 (1992)
- Verma, A.K., Mahajan, C.G.: *Indian J. Pure Appl. Phys.* **26**, 380 (1988)
- Vidal, T.H.G., et al.: *Mon. Not. R. Astron. Soc.* **469**, 435 (2017)
- Wakelam, V., Caselli, P., Ceccarelli, C., Herbst, E., Castets, A.: *Astron. Astrophys.* **422**, 159 (2004)
- Wakelam, V., Hersant, F., Herpin, F.: *Astron. Astrophys.* **529**, A112 (2011)
- Wang, N.X., Wilson, A.K.: *J. Phys. Chem. A* **109**, 7187 (2005)
- Wei, C., Zhang, X., Ding, D., Yan, B.: *Chin. Phys. B* **25**, 013102 (2016)
- Werner, H.-J., Knowles, P.J., Lindh, R., Manby, F.R., Schutz, M., et al.: *MOLPRO*, version 2012.1, a package of ab initio programs (2012). See <http://www.molpro.net>
- Whang, T.J., Wu, H.W., Chang, R.Y., Tsai, C.C.: *J. Chem. Phys.* **121**, 10513 (2004)
- Wigner, E., Witmer, E.: *Z. Phys.* **51**, 859 (1928)
- Wilson, A.K., Dunning, T.H. Jr.: *J. Chem. Phys.* **119**, 11712 (2003)
- Woon, D.E.: *J. Phys. Chem. A* **111**, 11249 (2007)
- Wright, J.J., Balling, L.C.: *Chem. Phys. Lett.* **108**, 214 (1984)
- Xing, W., Shi, D., Sun, J., Liu, H., Zhu, Z.: *Mol. Phys.* **111**, 673 (2013)
- Zhang, L.L., Gao, S.B., Meng, Q.T., Song, Y.Z.: *Chin. Phys. B* **24**, 013101 (2015a)
- Zhang, L.L., Zhang, J., Meng, Q.T., Song, Y.Z.: *Phys. Scr.* **90**, 035403 (2015b)